



Create the Future

Digital Commons @ Michigan Tech

Michigan Technological University

Dissertations, Master's Theses and Master's
Reports - Open

Dissertations, Master's Theses and Master's
Reports

2014

MICROWAVE ABSORPTION PROPERTIES OF TIRES

Yuzhe Zhang

Michigan Technological University

Follow this and additional works at: <https://digitalcommons.mtu.edu/etds>



Part of the [Materials Science and Engineering Commons](#)

Copyright 2014 Yuzhe Zhang

Recommended Citation

Zhang, Yuzhe, "MICROWAVE ABSORPTION PROPERTIES OF TIRES", Master's Thesis, Michigan Technological University, 2014.

<https://digitalcommons.mtu.edu/etds/889>

Follow this and additional works at: <https://digitalcommons.mtu.edu/etds>



Part of the [Materials Science and Engineering Commons](#)

MICROWAVE ABSORPTION PROPERTIES OF TIRES

By
Yuzhe Zhang

A Thesis

Submitted in partial fulfillment of the requirements for
the degree of

MASTER OF SCIENCE

In Materials Science and Engineering

MICHIGAN TECHNOLOGICAL UNIVERSITY

© 2014 Yuzhe Zhang

This thesis has been approved in partial fulfillment of the requirements for the Degree of MASTER OF SCIENCE in Materials Science and Engineering

Department of Materials Science and Engineering

Thesis Advisor: *Jiann-Yang Hwang*

Committee Member: *Bowen Li*

Committee Member: *Xinli Wang*

Department Chair: *Stephen L. Kampe*

Table of contents

List of Figures.....	5
List of Tables	7
Acknowledgements	8
Abstract.....	9
Chapter 1: Introduction	10
1.1 The waste tire	10
1.2 Methods for recycling waste tires.....	13
1.2.1 Landfill	13
1.2.2 Stockpiles	14
1.2.3 Pyrolysis.....	14
1.3 Microwave heating.....	16
1.3.1 Microwave fundamentals.....	17
1.3.2 Microwave heating principles	17
1.3.3 Non-thermal effect of microwave.....	17
1.3.4 The processing of microwave.....	19
1.4 Resistance furnace	19
1.5 The goal of this research	20
Chapter 2: Experiment	21

2.1 Material	21
2.2 Equipment	25
2.3 Principles	26
Chapter 3: Results and Discussion	31
3.1 Experiment in stagnant air	31
3.2 Experiment in nitrogen	46
Conclusion	61
References	63
Appendix I	68
Appendix II	69
Appendix III	70

List of Figures

Figure 1. Polar molecules in microwave field.....	18
Figure 2. General morphology of tire rubber sample (scale bar 100 μm).....	21
Figure 3. The elemental composition of area 1 of Figure 2.....	22
Figure 4. The elemental composition of area 2 of Figure 2.....	24
Figure 5. The elemental composition of area 3 of Figure 2.....	19
Figure 6. Diagram of the TM_{0n0} cavity system.....	25
Figure 7. Temperature dependences of sample density (gm/cc), sample volume (mm^3) and sample mass (gm) under stagnant air.....	32
Figure 8. Temperature dependences of sample length(mm) and 3-dsample (sample diameter/mm) under stagnant air.....	33
Figure 9. Temperature dependences of log(relative dielectric constant) under stagnant air.....	34
Figure 10. Temperature dependences of log(relative dielectric loss factor) under stagnant air.....	36
Figure 11. Temperature dependences of log($\tan\delta$) under stagnant air.....	38
Figure 12. Temperature dependences of log(half-power depth) under stagnant air.....	39
Figure13. Temperature dependences of log(penetration depth) under stagnant air.....	41
Figure 14. Temperature dependences of the reflection loss(dB) at 915MHz under stagnant air.....	43
Figure 15. Temperature dependences of the reflection loss(dB) at 915MHz under stagnant air.....	45
Figure 16. Temperature dependences of sample density(gm/cc), sample volume(mm^3) and sample mass(gm) under UHP nitrogen.....	47

Figure 17. Temperature dependences of sample length(mm) and sample diameter(mm) under UHP nitrogen.....	48
Figure 18. Temperature dependences of relative dielectric constant under UHP nitrogen.....	49
Figure 19. Temperature dependences of log(relative dielectric loss factor) under UHP nitrogen.....	50
Figure 20. Temperature dependences of $\tan\delta$ under UHP nitrogen.....	52
Figure 21. Temperature dependences of log(half-power depth) under UHP nitrogen.....	53
Figure 22. Temperature dependences of log(penetration Depth) under UHP nitrogen.....	55
Figure 23. Temperature dependences of the reflection loss(dB) at 915MHz UHP nitrogen.....	57
Figure 24. Temperature dependences of the reflection loss(dB) at 915MHz under stagnant air.....	59

List of Tables

Table 1. Composition of tire(wt%).	11
Table 2. Recycling of discarded tire in some countries and regions.	12
Table 3. Elemental composition of area 1.	22
Table 4. Elemental composition of area 2.	23
Table 5. Elemental composition of area 3.	24
Table 7. Summary of Experimental Results of Tire rubber at 915MHz under Stagnant Air.	67
Table 8. Summary of Experimental Results of Tire rubber at 2466MHz under Stagnant Air.	68
Table 9. Summary of Experimental Results of Tire Rubber at 915MHz under UHP Nitrogen.	69
Table 10. Summary of Experimental Results of Tire Rubber at 2466MHz under UHP Nitrogen.	70

Acknowledgements

Here, I would like to thank many people who have helped me throughout my master's degree studies at Michigan Technological University.

First of all, I want to take this occasion to thank my advisor, Dr. Jiann-yang Hwang, for his guidance, financial support, and encouragement throughout the project and for reviewing my thesis.

I would also like to thank Dr. Ron Hutcheon for helping me to perform dielectric characterization experiments. He gives me persistent instruction of the experiment. Without his encouragement and good guidance, this work cannot be accomplished.

Special thanks to Dr. Zhiwei Peng for reviewing my thesis.

I also need to thank Dr. Bowen Li and Dr. Xinli Wang for being my committee members.

I deeply appreciate the generous help from Matthew Andriese, Chenlong Zhang and Xin Yan for technical support on testing methods.

Finally, I would like to gratefully thank my lovely wife and my family. Without their support and encouragement, it is impossible for me to finish this work

Abstract

The waste tire is belonging to insoluble high polymer elastic materials. It takes hundreds of years to resolve the macromolecules of waste tire into the standard which does not pollute the environment. More and more waste tires are air stored which causes space occupation and mosquito-breeding in the places that will spread diseases. The disposal methods include landfill, stockpiles, dumping and incising into particles. However, all these methods are not technically and economically efficient. The trend for the development of waste tire treatment processes is low cost, on-site, and high product recovery at high energy efficiency.

In this project, microwave energy has been applied for treatment of the waste tire in laboratory scale. Experimental conditions were varied in order to find the optimum processing parameters such as temperature and atmosphere. The microwave absorption capability of waste tire rubber was investigated by measuring its dielectric properties from room temperature to 800°C in stagnant air and pure nitrogen atmospheres, respectively, at both 915 and 2466MHz. The dielectric parameters data increase steadily at temperatures below 400°C. At temperatures above 400°C, the relative dielectric loss factor and relative dielectric constant begin to decrease. This is due to the solid phase of tire rubber begins to transform to gas phase and the release of volatiles. The calculations of microwave half-power depth and penetration depth of waste tire rubber show that the pyrolysis process significantly improves the microwave absorption capability of the waste tire rubber at low temperatures. The calculated reflection loss of the waste tire rubber suggests that its maximum microwave absorption can be obtained when the rubber has a thickness of 25mm at 915MHz. The sample dimension has a significant effect on the overall performance of microwave absorption in waste tire during pyrolysis and thus on the efficiency of microwave waste tire rubber pyrolysis.

Chapter 1: Introduction

1.1 The waste tire

The waste tire is also called black pollution. With the development of automobile industry, the black pollution becomes worse. When auto transportation first began to use rubber tires, processing of waste tires has become a big problem for more than 100 years. According to statistics, more than 1.5 billion of waste tires are produced all over the world annually. Every year the waste tire production in USA is more than 0.3 billion. For cities, states and industries, processing of discarded tires in the United States is a dilemma. Research shows that two to five billion waste tires are held in landfills and stockpiles. The governmental agencies, municipalities, industrial corporations and community leaders have attempted to reduce the size of space for waste tire storage.

Waste tires have environmental and health problems. The scrap tires can take a lot of space. Most of the scrap tires are stored outside. With the sun and rain, the scrap tire can promote breeding of mosquito which can carry acute infectious germs. What's worse, the scrap tire can easily cause fire.

In the landfill, the waste tires cannot be biodegraded. In addition, whole tires tend to work their way to the top of the fill and can cause damage to the landfill cap or seal. As a result, waste tires cannot be stored in landfills. Many tires are dumped illegally, due to the cost of placing them in sanctioned dumpsites.

Under this situation, almost all states of United States have established laws and proposed legislation, or adopted proposals for gathering the waste tires. Many attempts have been made to decrease the pollution of waste tires. Many of these states collect license fees or taxes from factories and companies for processing the waste tire [1].

The compositions of waste tire are variable, depending on the manufacturer.

Table 1. Composition of tire (weight%) [2]

Materials		Element		Tire
name	Content	name	symbol	
Natural rubber	23	Carbon	C	73.0
Synthetic rubber	24	Hydrogen	H	6.0
		Oxygen	O	4.0
Carbon black	25	Nitrogen	N	1.4
		Sulfur	S	1.3
Steel cord	14	Chlorine	Cl	0.07
		Zinc	Zn	1.5
Weave cord	4	Iron Ashes	Fe	13.5
Others	10			

Table 1 shows the composition of tire. Rubber is a major component of the tire rubber and it is a kind of significant material because of it is one of the three main polymer material groups; natural rubber will be consumed is more than 15 million tons each year. More than 31 million tons of rubber will be produced globally every year. Amount of waste tires be produced each year is result from development of rubber industry. The waste rubber is major coming from waste rubber products which are manufactured from rubber process and others, such as: rubber shoes, waste tires, rubber pipes, edge scraps, rubber belts and waste products. The number of waste tires reaches 10 million every year worldwide and the recycling technologies of waste rubber are changing every day.

Table 2. Recycling of discarded tire in some countries and regions [2]

Place	Year	Amount (10000 Tons)	Disposing					
			Thermal- utilizing	Making powder	Regenerated rubber	Renew	Export	Burying
US	1992	280	23	6	4		3	63
Japan	1992	84	43		12	9	25	8
Germany	1993	55	38	14	1	18	18	2
British	1992	45	9	6		18		67
EEC	1990	197.5	30		20			50

Comprehensive utilization of waste tires are paid close attention by developed countries for reaching a target of resources recycling and environment protection. It is significant for waste rubber to be recycled. For instance, it can protect the environment. The reason is that the waste rubber causes more and more environmental pollution. Pets and mosquitoes are abundant around waste tire which is a good place for propagation. This condition can cause spreading of infections, for example, malaria, cephalitis and so on.

For countries, recycle of the waste tire can save the energy, because the raw material for the rubber industry depends on petroleum has to be great extent. This is particularly important for the countries which have little resources of natural rubber. These countries also use amount of waste tire rubber for producing raw materials. The waste rubber has the highest burning value of about 3.3×10^4 kJ/kg in the industrial division so that waste rubber is a kind of high-value bunkers the same as coal. Previous work shows that the world would lost 3×10^{14} kJ heat without recycling rubber [2]. It is very important to recycle waste rubber because there is a decrease of natural energy resources. The waste rubber is used as raw materials of industry. The

comminuted rubber and recycled rubber are produced from waste rubber so that they become raw material of the rubber industrial. In this condition, more and more attention has been paid to recycle of waste rubber. Consequently, waste tires which contain a lot of waste rubber, attracted much attention from scientists.

1.2 Methods for recycling waste tires

1.2.1 Landfill

The landfill method is a method which buries waste tires. It is the oldest method for treating waste materials. It can also be called as tip, dumping ground or rubbish dump. In history, landfill is the most normal way for the organization of waste charge all over the world.

However, landfill is not suitable for waste tire treatment. Due to their large volumes and 75% void space, they consume space rapidly [3]. The waste tire may produce buoyant bubble son the surface since they are able to trap methane gases. The buoyant bubbles can damage the landfill liners which have been installed to promote prevent landfill wastes to pollute the surface and ground water.

The landfill of waste tires can lead to a lot of problems. It just buries the waste tires without reuse so it is a waste of potentially valuable waste tires, although it is relatively easy to get and cheap for disposal purposes. The waste tires emit dioxins (toxic hydrocarbon), zinc oxide poly-nuclear aromatic hydrocarbons i.e. potent carcinogens, due to the fact that it can cause a serious fire disaster, leading to pollution of air. It is thus necessary to make use of this energy for electricity generation and to recover useful by-products such like char and steel, etc. taking use of new process, for example, by incineration and by pyrolysis which involves use of microwave heating or electric heating [5-10].

1.2.2 Stockpiles

The stockpiles of waste tires can make serious safety and health risks. Waste tires are able to appear easily and seriously polluting the air and ground. The waste tire has another risk of health that it provides places for vermin and mosquitoes for breeding resulting in an increasing number of diseases. The stockpiles also can cause illegal dumping of waste tires. The illegal dumping of waste tires makes many states to pass waste tire regulation requiring suitable managing because it will pollute woods, deserts, ravines and empty lots. All of the organization members are able to dispose a limited number of waste tires free of charge and this can be funded by state waste tire programs. As a result of this illegal dumping [11], improper storage of waste tires may be increased. This activation is sometimes related to illegal activities and lack of environmental awareness.

1.2.3 Pyrolysis

The word “pyrolysis” is derived from the separation of Greek-derived elements pyro “fire” and “lysis”. Pyrolysis involves thermochemical dissolution of organic material at raised temperatures with no oxygen or halogen. The pyrolysis is non-reversible and it includes immediate changes of physical phase and chemical composition [12].

The pyrolysis is commonly found in organic materials at high temperatures and it is a kind of thermolysis. The pyrolysis is one of the processes including wood charring that starts at the temperature from 200 to 300°C. As usual, gas and liquid are produced by pyrolysis of organic materials and it also leaves behind a solid residue which has high carbon content. In extreme conditions which carbonization takes place, the pyrolysis will leave behind most of carbon as the residue [12].

Pyrolysis widely used in chemical industry, such as producing activated carbon, methanol, charcoal and other chemicals from wood. It is used to make coke from coal and to convert biomass into biochar and syngas. What's more, the process converts ethylene dichloride into vinyl chloride to produce polyvinyl chloride. The public use pyrolysis to make wastes become safely disposable products and to convert medium-weight hydrocarbons into gasoline. In view of these functions, pyrolysis is also called destructive purification or fracture.

The pyrolysis differs from other high-temperature processes, such as hydrolysis and combustion, because pyrolysis often includes reactions with no water and oxygen. Actually, it is impossible to get a totally anaerobic atmosphere. Pyrolysis of waste tires can make the solid in the tire out. For example, carbon black, steel and carbon, from volatile liquid and gaseous compounds that can be used as fuel [11]. The pyrolysis of waste tire has been widely used all over the world.

The pyrolysis way for waste tire recycling is a technology which heats particles or whole of waste tire in a reactor in anaerobic environment. Waste tires will be decomposed into small particles and become softened in the reactor. These particles will vaporize and emit from the reactor at the end of the process. The vapors are usually used as fuel that is burned directly for producing energy. Some particles which are not big enough for condensing remain as gas for burning as fuel. Some parts of waste tire which are about 40% by weight are removed as solids [11]. The pyrolysis of waste tire process can be very clean without waste or emissions.

The raw materials used and the process conditions determines the properties of the solid, gas and liquid output. For example, whole waste tires include steel and fibers. Most of the steel are owned by the waste tires which are shredded and most of the fiber is removed. The processes can be continuous or discontinuous [11]. The power needed to drive the dissolution of waste tires may be directly produced by fired

fuel or microwaves, or electrical induction. A catalyst is sometimes used to improve the speed of the dissolution.

The comparison of different methods for waste tires recycling shows that pyrolysis is the best choice. Some work on the recycling of waste tires has already been reported [13-18]. However, in fact, there still has many operational problems related to the models used on the market so that further effort need to be done.

Pyrolysis has a lot of advantages. First of all, pyrolysis is safe and convenient because no complex operations (e.g., slag removal) are needed. Both of the speed of pyrolysis and incineration can be controlled [11]. Then it can make secondary distribution of heat generated by waste tire so that it improves secondary burning and save fuel.

Secondly, the organic compositions of waste tire can be transferred to be a useful form of energy in the process of pyrolysis so that it is more economic. According to its calorific value, the gas which is produced by pyrolysis can be fired straightly or be fired after mixing with other higher calorific value fuels. The tar which is produced during this process can be made to be fuel or chemical raw material in line with its properties [11].

Thirdly, pyrolysis system has less secondary pollution so that the problem of pollution can be simplified. It will be safer for environment. The reason is that materials is processed under anaerobic conditions so it will produce less harmful substances such as NO_x, SO_x and HCl. The pyrolysis can produce gas which can be fired under low air condition, generating less waste gas. In this condition, pyrolysis has less air pollution and it can lower the level of secondary pollution discharging [11]. So pyrolysis is a safe method for processing waste tire.

1.3 Microwave heating

1.3.1 Microwave fundamentals

Microwave is a kind of electromagnetic wave having the frequency from 300MHz to 300GHz. Microwave also has corresponding energies from 1.24×10^{-6} to 1.24×10^{-3} eV [19]. Compared to the normal ionization energies, the corresponding energies of microwave is much lower. The law of optics is the one which microwave obeys. Microwaves can be transmitted, absorbed and reflected. There are three kinds of materials according to various interactions between materials and microwave: opaque materials, absorbers and transparent materials. The opaque materials are able to not allow wave spread and reflect microwave (e.g., most metals). The absorbers can absorb various waves. The transparent materials only have little reciprocity with microwave. Be based on the materials properties, absorbers can be heated by microwave under different temperature [19].

1.3.2 Microwave heating principles

Microwave heating is a kind of heating more advancing than traditional heating. The reason is that materials absorb microwave energy volumetrically and microwave energy can be absorbed at molecular level by materials. There are four loss mechanisms: conduction, hysteresis, resonance which is also called magnetic loss, and dipolar polarization.

1.3.3 Non-thermal effect of microwave

Some experimental work found the non-thermal effect of microwave field. The activation energy which is generated through orientation effects of molecules (entropy effect) may be lowered by the microwave field. This is because microwave has high acceleration of reaction rate. As a result, the microwave can also lower the storage energy which is the same as oscillatory energy of molecules (enthalpy effect).

But this effect can't be confirmed so far. Unlike traditional synthesis, the microwave assisted synthesis hardly controls some experiments conditions like pressure and temperature. This situation becomes even worse without accurate and reliable temperature measurement techniques [19]. To ensure the existence of the non-thermal effect, the quantitative evaluations are necessary.

With the ability of the electric field to polarize the electric charge of the stuff where polarization cannot follow the changing electric fields, microwave can heat dielectric materials. There are four important kinds of dielectric polarization: The first one is orientation polarization. This kind of polarization is resulted in by the reorientation of the constant dipoles because of the influencing electric field. The second one is electron polarization. This kind of polarization is because of the position changes of electrons around the nucleus. The third one is spatial charge polarization. This kind of polarization is found when materials consisting of free electrons whose allocation are limited by the surface of grain. The fourth one is atomic polarization. This kind of polarization is produced by the nucleus positional shifting because of the asymmetry allocation of the charge within the molecule.

Figure 1 shows how polar molecules reorient in a microwave field.

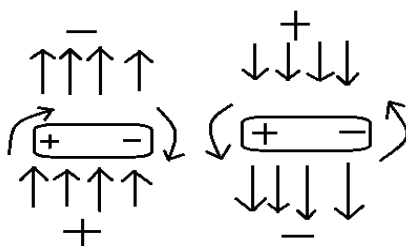


Figure 1. Polar molecules reorient in microwave field

Orientation (dipole) polarization is the most vital mechanism in microwave frequency range because electron and atomic polarization require much more energy than the energy which can be produced at microwave frequency [21].

Another important microwave heating mechanism is ionic conduction. Due to their native charge, the ions of a solution move under microwave field and collide. The collisions will lead to transformation of kinetic energy to thermal energy. There are an increasing number of collisions with the increasing concentration of ions in solution so that the solution will be heated faster at higher concentration.(Schaefer,1999) [21].

There are three kinds of materials which are classified based on the response to microwave heating: The first kind is conductors which prevent microwave penetrating and reflect microwaves [21]. The second kind is high loss or absorbing materials. This kind of material absorbs the microwave and then convert electromagnetic energy to heat.

1.3.4 The processing of microwave

Because of the great advantage of microwave, it has been paid more attention and be used as an advancing heating source. The advantages of microwave processing include:

- a. Stopping and start-up quickly
- b. Heating can be selective for materials
- c. Has a high-level of automation and safety
- d. Heating without contact
- e. Non- thermal effect: reaction's activation energy can be lowered
- f. Less process time and consumption of energy
- g. Heating is volumetric and rapid

1.4 Resistance furnace

The resistance furnace is also called electric furnace. It is a furnace in which the

heat is produced by the part of current through an appropriate inside resistance which is possible the charge itself. It has a resistor surrounding the charge or a resistor embedded in the charge [20].

The resistance furnace has a variety of advantages so that it is widely used. The furnace has a chamber which is able to get any temperature up to 3000°C[20]. The power control can be automatic so that it is easy to control temperature in such a furnace. The resistance furnace can be automatic and mechanized so that it can promote the inclusion of such furnaces in automatic transfer lines or alleviate the work of people[20]. What's more, the resistance furnace is compact and can offer a safe environment for many types of processes. The resistance furnace proper is well sealed to achieve a high vacuum.

1.5 The goal of this research

The thesis is aimed to determine microwave absorbing capability of the tire rubber with changing temperature and experiment atmosphere. The results may provide a useful guide for waste tire recycling.

Chapter 2: Experiment

2.1 Material

The waste tire sample was purchased from the Cooper Company, Michigan. It has the following description: 104T max load 900kg (2984 LBS), max press 300kg (44 P.S.I), tread 1 PLY NYLON + 2 PLY STEEL + 2 PLY POLYESTER, sidewall 2 PLY POLYESTER , made in USA, tread wear 700, traction A, temperature B.

The samples were prepared by cutting off rubber rods from the center of tire tread. These rods have a length of 12 mm, diameter 7 mm.

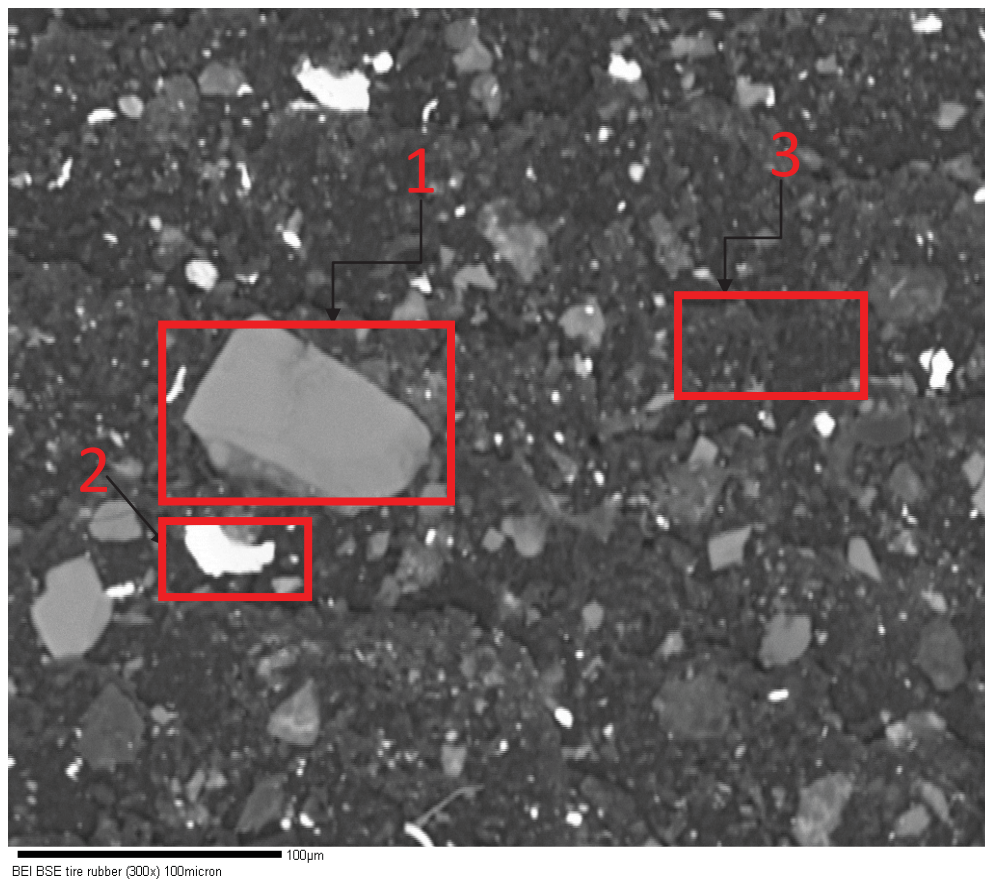


Figure 2. General morphology of tire rubber sample (scale bar 100 μm)

Figure 2 shows a SEM micrograph of the waste tire rubber. The large gray grain to the left is designated as Area 1. The bright grain below the Area 1 is named Area 2. The groundmass with large amounts of small aggregates at the center right part of the

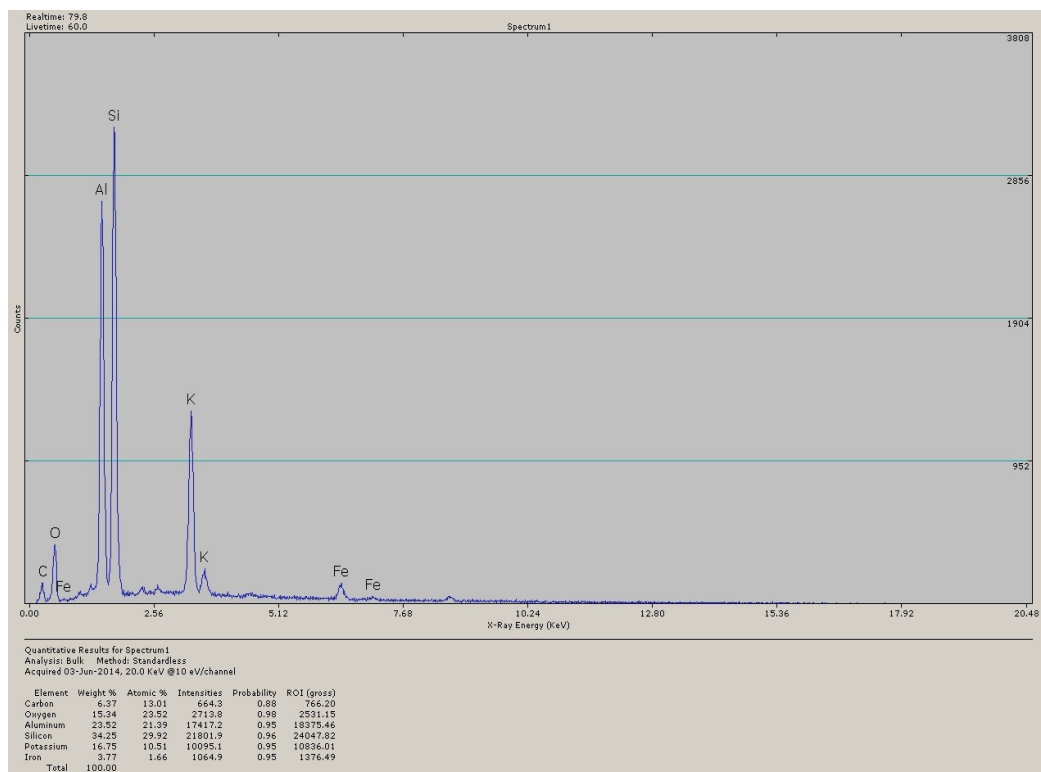


photo is Area 3. The three areas were analyzed with EDAX for their compositions.

Figure 3. Elemental composition of area 1 in Figure 2

Table 3. Elemental composition of area 1

Element	C	O	Al	Si	K	Fe
Weight%	6.37	15.34	23.52	34.25	16.75	3.77

The table 3 shows the result of the elemental composition of area 1. The area 1 contains 6.37 weight% C, 15.34 weight% O, 23.52 weight% Al, 34.25 weight% Si, 16.75 weight% K and 3.77 weight% Fe. It indicates that the area 1 may represent a

filler particle in the rubber. The chemical composition of this grain is clearly a potassium aluminum silicate, which is most likely a feldspar mineral. In the tire description earlier from the manufacture, it didn't mention that silicate minerals are part of the tire. However, it is common to have mineral filler in the organics for cost reduction. We believe that tire manufacturers are also use mineral fillers as a cost reduction approach. So, this grain may represent a typical mineral filler grain.

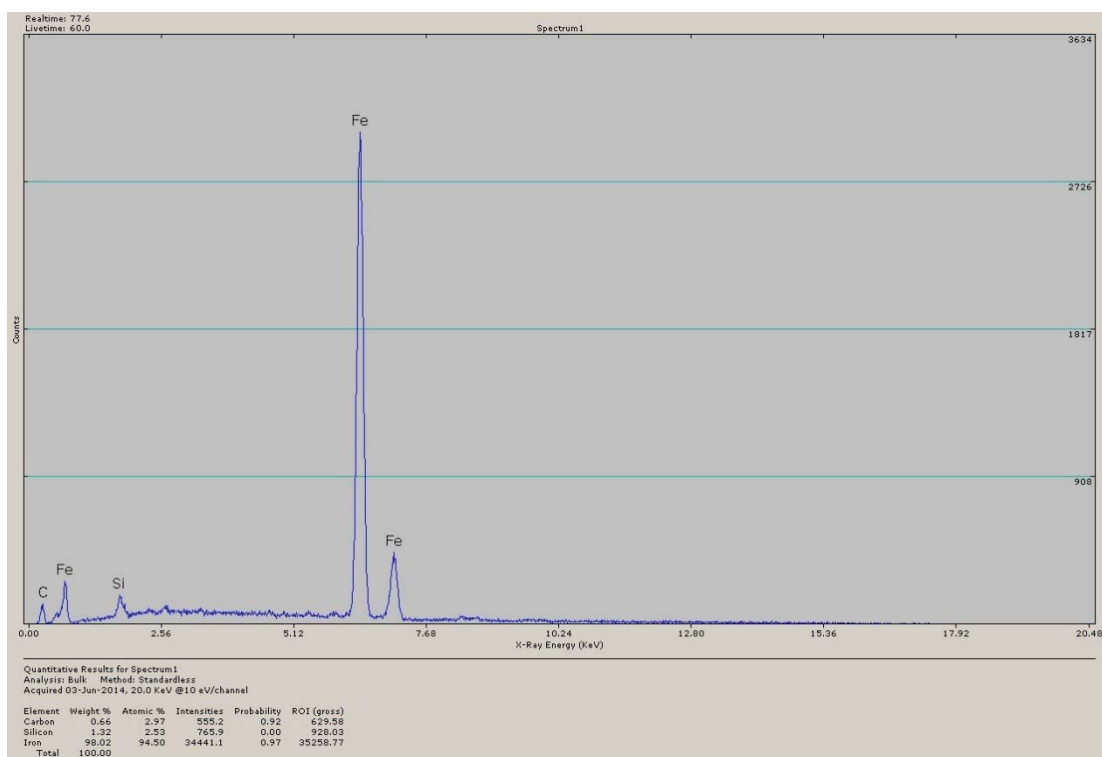


Figure 4.The elemental composition of area 2 of Figure 2

Table 4. Elemental composition of area 2

Element	C	Si	Fe
Weight%	0.66	1.32	98.01

Table 4 shows the results of elemental composition of area 2. The area 2 contains 0.66 weight% C, 1.32 weight% Si and 98.01 weight% Fe. The maximum composition

of area 2 is Fe and most of area 2 is Fe. The area 2 is primarily iron, which is obviously the steel reinforcement in rubber.

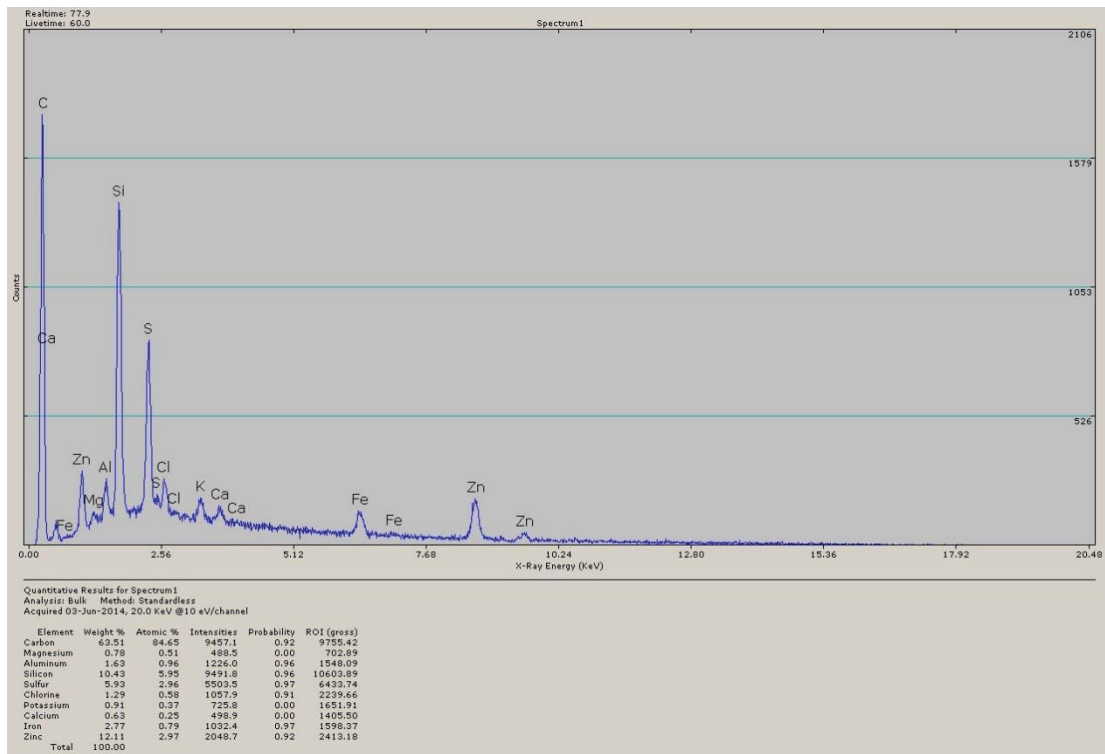


Figure 5. The elemental composition of area 3 of Figure 2

Table 5. Elemental composition of area 3

Element	C	Mg	Al	Si	S	Cl	P	Ca	Fe	Zn
Weight%	63.51	0.78	1.63	10.43	5.93	1.29	0.91	0.63	2.77	12.11

Table 5 shows the results of elemental composition of area 3. The area 3 contains of 63.51 weight% C, 0.78 weight% Mg, 1.63 weight% Al, 10.43 weight% Si, 5.93 weight% S, 1.29 weight% Cl, 0.91 weight% P, 0.63 weight% Ca, 2.77 weight% Fe and 12.11 weight% Zn. The maximum composition of area 3 is C. The area 3 should contain carbon black, natural rubber. The composition of area 3 is primarily carbon, about 63% of the total weight. This area represents the groundmass of the material,

and is thus the typical rubber dominant part of the material. The presence of sulfur (5.93%) for rubber vulcanization and zinc (12.11%, in form of zinc oxide actually) as the activator for rubber vulcanization reaction prove that this area is the rubber area.

2.2 Equipment

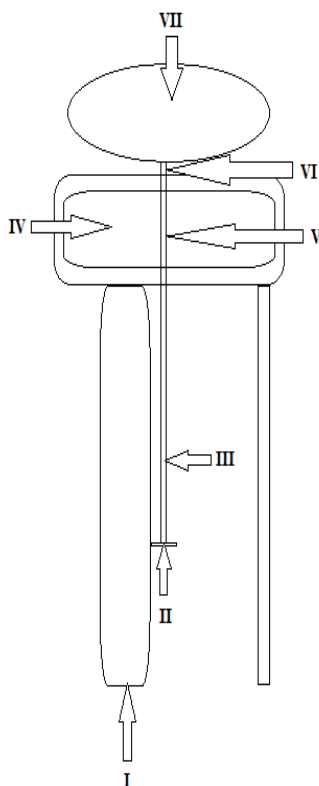


Figure 6. Diagram of the TM_{0n0} cavity system

Figure 6 shows the linear actuator with a sample lined in axis in the middle of the cavity and the quartz sample holder. There is a small hole in the quartz base which supports the sample in the holder so that gas can flow upwards using a (not shown) metered gas flow control system.

The system is consisted of: (I) support stand, (II) sample stage on linear actuator,

(III) quartz sample holder, (IV) TM_{0n0} right cylindrical cavity, (V) sample in quartz holder, (VI) entry hole and (VIII) high temperature resistance furnace.

2.3 Principles

Depending on the frequency and temperature range the equation for describing the dielectric response of a substance is related to the permittivity (ϵ) for non-magnetic dielectrics, which can be shown as

$$\epsilon = \epsilon_0 \epsilon_r = \epsilon_0 (\epsilon_r' - j\epsilon_r'') \quad (1)$$

Where ϵ_0 is the permittivity of free space (8.8854×10^{-12} F/m), and j is imaginary unit where $j^2 = -1$. The symbol ϵ_r is complex relative permittivity and it is used to describe the constitutive relation between the electric field intensity in loss dielectrics and the electric flux density. The symbol ϵ_r is consisted of two parts: one is ϵ_r'' which is the relative dielectric loss factor or imaginary part of complex relative permittivity. The other is ϵ_r' which is the relative dielectric constant or real part of complex relative permittivity. Although the imaginary part of complex relative permittivity represents the loss of electrical energy in dielectrics, the real part of complex relative permittivity is a measure of the ability of the dielectrics to stock electrical energy. The energy lost from the electric area to the dielectric is finally transformed to heat or thermal energy. As a result, the imaginary part of complex relative permittivity determines the rate of heating when applying microwave energy for dielectrics with no magnetic response.

It was assumed that the free electron conductivity mainly caused the dielectric loss, and the final-state dielectric loss factor was assumed at room temperature by measuring the dc resistance of the heated sample. The theoretical relationship between the dielectric loss factor and the dc resistance is:

$$\varepsilon'' = \frac{1}{2\pi f \varepsilon_0 R \left(\frac{\pi D^2}{4L}\right)} (2)$$

In this equation R is the resistance measured in the experiment, the f is the frequency of microwave, the L is the sample length and the D is the diameter of the sample. The value of dc resistance was used to calculate a theoretical dielectric loss factor. Then the dielectric loss factor was compared with the measured dielectric loss factor for testing of the microwave loss mechanism.

In this research, the cavity perturbation technique was used to measure the dielectric properties (ε_r' and ε_r'') of the tire rubber during pyrolysis at frequency of 915 and 2466MHz. This technique measures the differences which are changes in quality factors and shifting frequency caused by the microwave cavity response between the cavity with a sample –holder plus the sample and the same cavity with an empty sample-holder. Then calculation of the permittivity needs to use these differences.

The experiments have two runs. The first experiment was done in stagnant air. The second experiment was done in ultra high pressure nitrogen which can avoid the oxidation and combustion of the waste tire rubber sample.

The first experiment was done in stagnant air with a short sample holder which is 80mm high.

During the experiments, the waste tire rubber sample was run consisted of measurements at room temperature (RT). The temperature was starting at 25°C then increased in 25°C steps to 725°C. Then the temperature was cooled 100°C steps to room temperature which is 25°C. After the measurement, the waste tire rubber sample mass was measured immediately. Then the waste tire rubber sample was removed and the temperature of holder was measured up to 725°C. There is no contamination in the holder.

The second experiment was done under 20 psig nitrogen with a long holder

which is 500mm high.

The run was started by loading the waste tire rubber sample into the holder, then flushing the holder with nitrogen using a long tube inserted down into the holder. Then pressurizing and sealing the holder at 20 psig nitrogen.

The run was consisting of temperature measurements starting at room temperature (RT) 25°C. Then the temperature was increased in 25°C steps to 400°C, where the sample could be viewed quickly and looked completely normal. The run was continued up to 750°C. Then the temperature measurements were decreasing with 100°C steps to 25°C. The waste tire rubber sample could not be removed at the end of the run, and there was a black coating on the inside of the holder up to 140mm above the sample.

All of the measurement sequences were programmed with temperature calibration in the furnace, movement of the linear actuator (Figure 6). A personal computer running lab view control software controlled all of the network analyzer analysis.

As shown in Figure 6, a cylindrical TM_{0n0} resonant mode cavity (ø 580mm × 50mm) and a resistive heating furnace are the main parts of the measurement system. The top part of the holder involving sample was raised in the furnace and held at least 5 min to make sure that the sample reach the equilibrium furnace temperature for measuring the permittivity at a specific temperature. Next, the holder with no sample lowered into the central maximum electric area region of the thick-walled, well-cooled copper TM_{0n0} cavity quickly with the time small than 1.5s for each frequency. The frequency shift Δf and the quality factor Q because of the sample insertion were recorded in a Hewlett-Packard 8753B vector network analyzer.

The electric susceptibility ($\chi_e = \chi_e' - j \chi_e''$) with the data of the quality factor Q was calculated by the equation:

$$\frac{\Delta f}{f_e} + j \left[\frac{1}{2Q_{L,S}} - \frac{1}{2Q_{L,S}} \right] = \frac{-\chi_e}{1+F_{sh}\chi_e} \left[\frac{V_s}{V_c} \right] A(3)$$

In this equation the Δf is the frequency shift which is included by the sample, the f_e is the special cavity mode frequency which is 915 or 2466 MHz, $Q_{L,S}$ is the loaded cavity quality factor with the empty holder, V_c and V_s are the volumes of respective cavity and sample, F_{sh} is a real number which is based only on the shape of sample and A is a real calibration constant which is based only on the shape of electric areas in the absence of sample. The dielectric loss factor (ϵ_r'') and relative dielectric constant (ϵ_r') could be calculated after the susceptibility was determined.

In this research we also need to study about the Half- Power Depth. The Half-Power Depth is a parameter to evaluate the microwave absorption ability of materials. It is defined as the distance from the surface into the materials at which the traveling wave power drops to 1/2 from its value at the surface. The equation is [22]

$$D_{halfP} = \left(\frac{\ln 2}{2} \right) - (\text{inverse } \alpha)(4)$$

Where the inverse α is the TEM mode attenuation constant in the material. The equation of inverse α is:

$$\text{inverse } \alpha = \frac{2.998 \times 10^{10}}{2\pi f_e \times 10^6} \times \left\{ \frac{2}{[\sqrt{1+(\tan \delta)^2}] - 1} \times \epsilon_r' \right\}^{\frac{1}{2}}(5)$$

Where the f_e is the specific cavity mode frequency of microwave (915 or 2466MHz), $\tan \delta = \frac{\epsilon_r''}{\epsilon_r'}$.

The penetration depth D_p is a parameter to evaluate the microwave absorption ability of materials. It is defined as the distance from the surface into the materials at which the traveling wave power drops to $\frac{1}{e}$ from its value at the surface. The penetration depth can be calculated from the dielectric loss factor and the relative dielectric constant:

$$D_p = \frac{\lambda_0}{2\pi(2\epsilon_r')^{\frac{1}{2}}} \left\{ \left[1 + \left(\frac{\epsilon_r''}{\epsilon_r'} \right)^2 \right]^{\frac{1}{2}} - 1 \right\}^{-\frac{1}{2}}(6)$$

Where λ_0 is the wavelength of the microwave in free space.

The reflection loss calculation is also needed for this research. Since microwave heating is generally conducted in a metallic cavity, the reflection loss RL can be employed to further analyze the microwave absorption ability of sample. The equation is:

$$RL = 20 \log \frac{\left| \sqrt{\frac{\mu_r}{\epsilon_r}} \tanh \left(j \frac{2\pi f}{c} \sqrt{\mu_r \epsilon_r} d \right) - 1 \right|}{\left| \sqrt{\frac{\mu_r}{\epsilon_r}} \tanh \left(j \frac{2\pi f}{c} \sqrt{\mu_r \epsilon_r} d \right) + 1 \right|} \quad (7)$$

Where μ_r is complex relative permeability of sample and its value is assumed to be 1 in the calculation of reflection loss of coal and d is thickness of sample. The c is the velocity of microwave in free space.

Chapter 3: Results and Discussion

3.1 Experiment in stagnant air:

The measurement was performed in stagnant air using a short (~ 80 mm high) sample holder.

The initial sample parameters were:

- a) Diameter: 3.60 ± 0.15 mm
- b) Length: 13.59 ± 0.05 mm
- c) Mass: 0.153 ± 0.002 gm
- d) Room temperature density: 1.11 ± 0.07 gm/cc.

The final sample parameters were:

- a) Diameter: 3.4 ± 0.15 mm
- b) Length: 12.4 ± 0.05 mm
- c) Mass: 0.059 ± 0.002 gm
- d) Room temperature density: 0.52 ± 0.05 gm/cc.

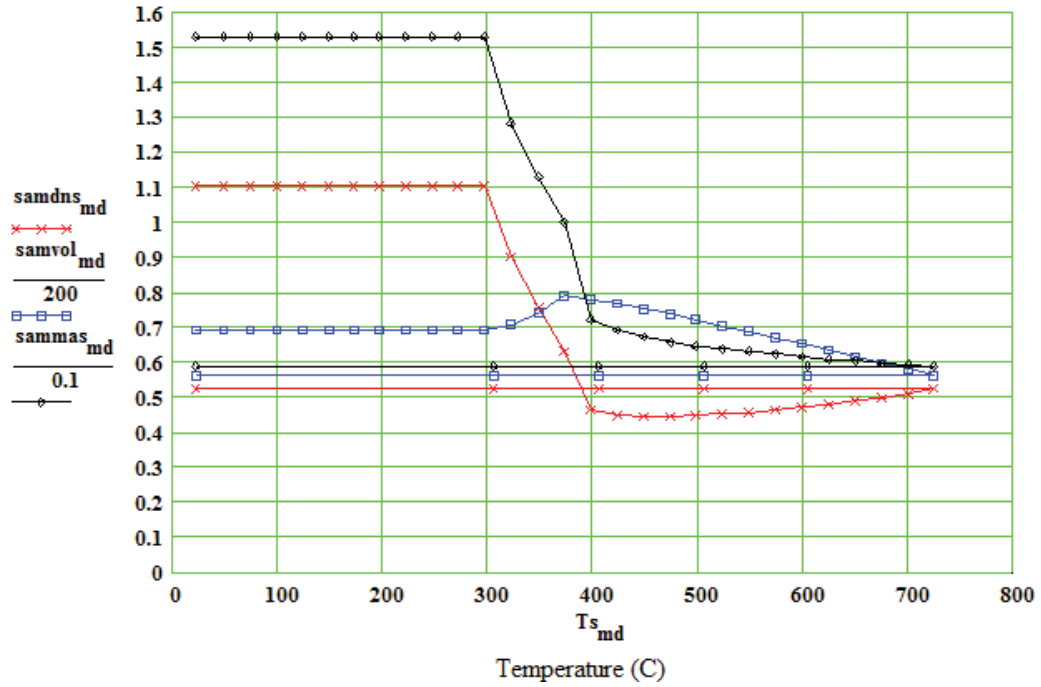


Figure 7. Temperature dependences of sample density (gm/cc), sample volume(mm³)and sample mass (gm) under stagnant air. The samdns_{md} is sample density, the samvol_{md} is sample volume and the sammas_{md} is sample mass.

Figure 7 shows that the variation of sample density can be separated into four distinct stages. The sample density is stable in the range of room temperature to 300°C. There is a substantial decrease in the density from 300 to 400°C. Then sample density keeps increasing slowly in the range of 400 to 800°C. The sample volume behaves similarly to the sample density at the beginning. But the sample volume increases in the range of 300 to 400°C and then it keeps decreasing in the range of 400 to 800°C. The sample mass behaves similarly to the sample density. The only difference is that the sample mass keeps decreasing slowly in the range of 400 to 800°C.

Figure 7 also shows sample volume, sample density and sample mass are

dependent on temperature. With the temperature increasing, some parts of tire rubber transform to liquid and gas so that the sample volume is increasing and the sample mass is decreasing in the range of 300 to 400°C. The rate of sample mass decreasing is faster than the rate of volume increasing so the sample density is decreasing in the range of room 300 to 400°C. The liquid is evaporated so the sample volume decreases and the rate of volume decreasing is larger than rate of sample mass decreasing. Hence, the sample density is increasing in the range of 400 to 800°C.

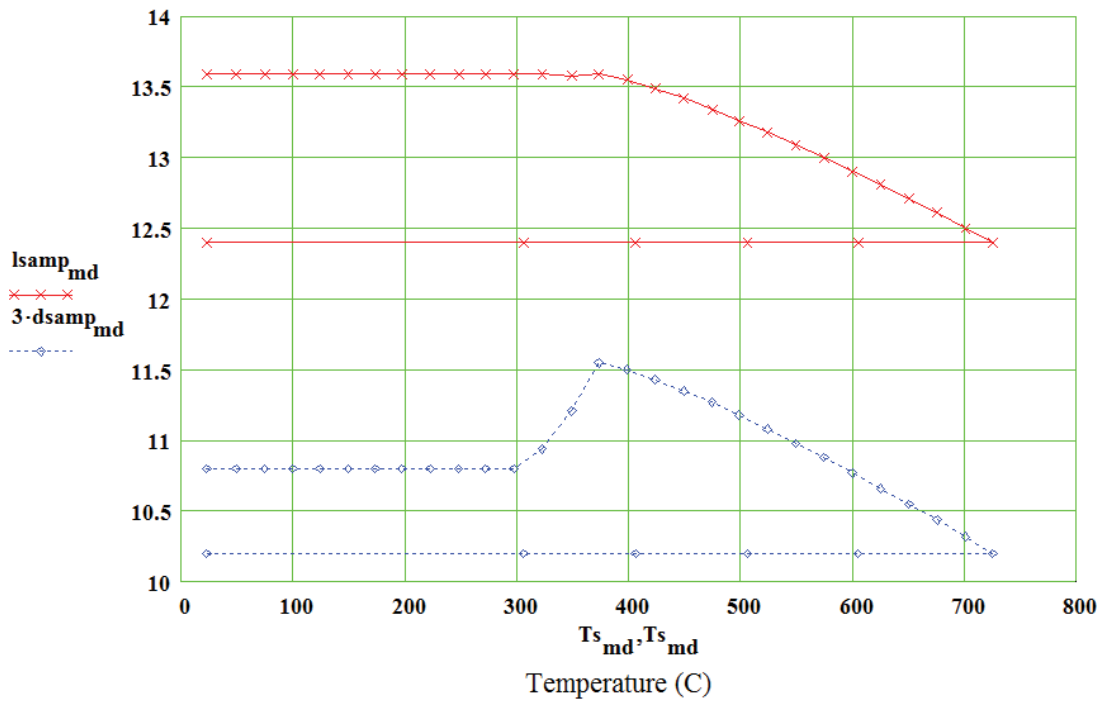


Figure 8. Temperature dependences of sample length(mm) and sample diameter(mm) under stagnant air. The $l_{s_{amp}_{md}}$ is sample length and the $3 \cdot d_{s_{amp}_{md}}$ is sample diameter.

Figure 8 shows that the variation of sample length can be separated into three different stages. The sample length is stable in the range of room temperature to

400°C. It keeps decreasing in the range of 400 to 800°C. The variation of sample diameter can be separated into four distinct stages. It is stable in the range of room temperature to 300°C. Then the sample diameter increases in the range of 300°C to 375°C. Finally the sample diameter keeps decreasing.

Figure 8 shows the temperature dependences of sample length and sample diameter. Some parts of tire rubber transform to liquid and gas so that length is decreasing when the temperature is increased. But some liquid is viscous and may adsorb on the side of sample. As a result, the sample diameter keeps increasing in the range of 300 to 400°C.

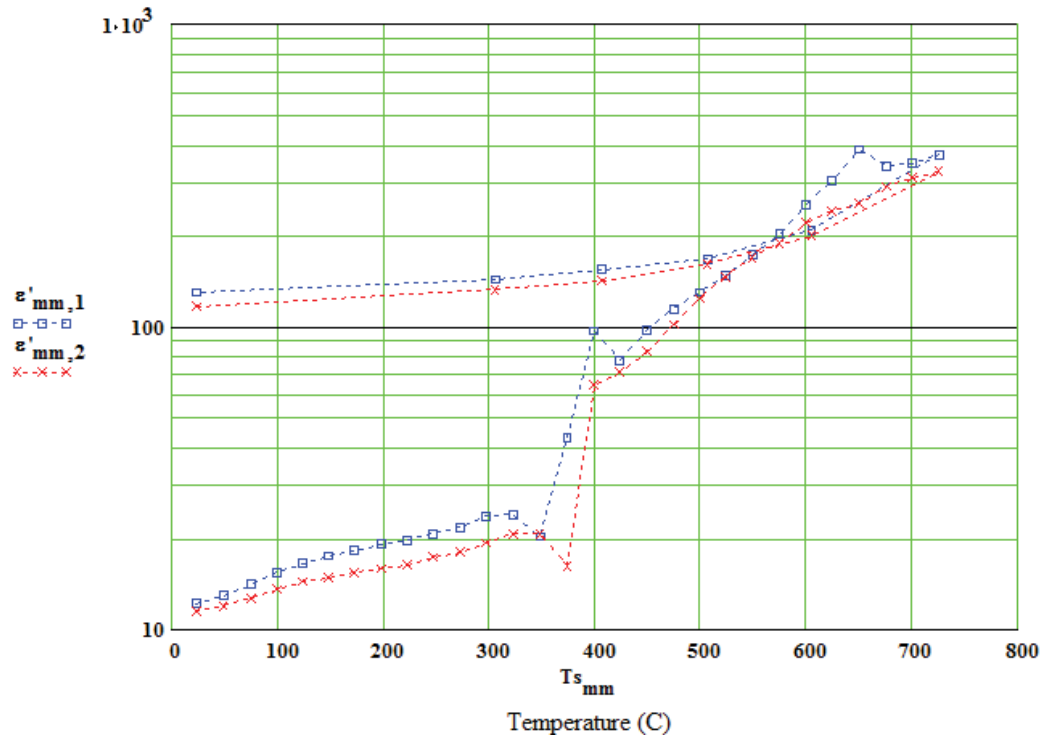


Figure 9. Temperature dependences of log(relative dielectric constant) under stagnant air. The $\epsilon'_{mm,1}$ is the log(relative dielectric constant) at 915MHz, the $\epsilon'_{mm,2}$ is the log(relative dielectric constant) at 2466MHz.

Figure 9 shows that variation of relative dielectric constant of tire rubber at

915MHz can be separated into five distinct stages. It keeps increasing in the range of room temperature to 650°C. It decrease firstly, then it keeps increasing from 650 to 800°C. The relative dielectric constant of tire rubber at 2466MHz behaves similarly to the relative dielectric constant of 915MHz. The relative dielectric constant of tire rubber at 915MHz is higher than that at 2466MHz.

As seen in Figure 9, although relative dielectric constant of tire rubber at 915MHz is higher than the relative dielectric constant of tire rubber at 2466MHz, the relative dielectric constant of the tire rubber is independent of the microwave frequency. In the tire rubber, the main component which absorb microwave is carbon black because the carbon black has strong polarity [22]. With the temperature increasing, the pyrolysis of tire rubber produces more carbon black so the content of carbon black increases in the products. As a result, the microwave absorption capability of sample becomes stronger. The relative dielectric constant increases with temperature. The relative dielectric constant is in direct proportion to the temperature. The relative dielectric constant indicates the polarity of tire rubber molecules. The increased relative dielectric constant implies stronger polarity of sample. The microwave absorption in tire rubber gets better in the range of room temperature to 800°C.

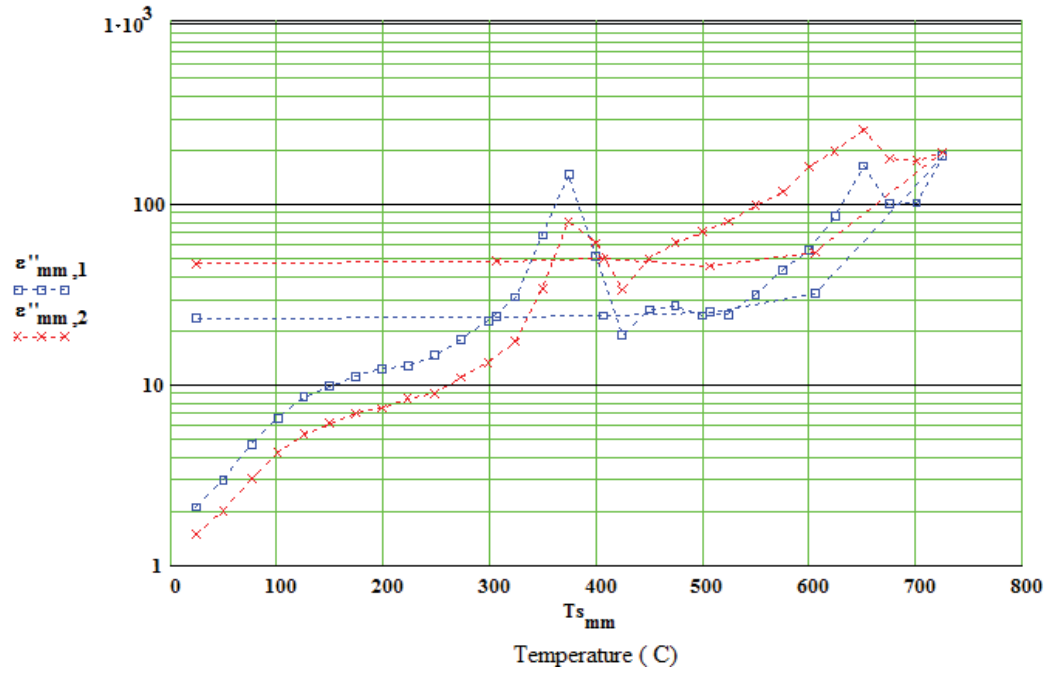


Figure 10. Temperature dependences of log(relative dielectric loss factor) under stagnant air. The $\epsilon''_{mm,1}$ is the log(relative dielectric loss factor) at 915MHz, the $\epsilon''_{mm,2}$ the log(relative dielectric loss factor) at 2466MHz.

Figure 10 shows that the relative dielectric loss factor of tire rubber varies with temperature at 915MHz. The variation can be separated into five distinct stages. It keeps increasing in the range of room temperature to 366°C, followed by a substantial decrease in the range of 366 to 415°C, and then an increase is in the range of 415 to 470°C. Then the relative dielectric loss factor of tire rubber at 915MHz decreases. There is a substantial increase in the range of 520 to 650°C. Afterwards, the relative dielectric loss factor of tire rubber at 915MHz decreases in the range of 650°C to 700°C. It is increasing in the range of 700 to 800°C. The relative dielectric loss factor of tire rubber at 915MHz behaves similarly to the relative dielectric loss factor of tire rubber at 915MHz. The relative dielectric loss factor of tire rubber at 915MHz is

higher than that at 2466MHz in the range of room temperature to 400°C. However, the relative dielectric loss factor of tire rubber at 915MHz is lower than the relative dielectric loss factor of tire rubber at 2466MHz in the range from 400 to 800°C.

Figure 10 shows that the relative dielectric loss factor of tire rubber at 915MHz is smaller than the relative dielectric loss factor of tire rubber at 2466MHz in the temperature range. The relative dielectric loss factor does not fit the equation $\epsilon'' = \frac{1}{2\pi f \epsilon_0 R \left(\frac{\pi D^2}{4 L} \right)}$, so that the microwave loss mechanism for pyrolyzed tire rubber is not pure free electron conduction. With temperature increasing, the increasing content of carbon black causes an increase in the relative dielectric loss factor. However, little air in container can react with carbon black. There is an obvious dielectric loss peak in the range of 300 to 400°C. This is a typical interfacial/relaxation polarization phenomena behavior, usually indicating a change in the material associated with the loss of an insulating barrier [22]. It indicates a phase transformation and the product do not absorbs microwave well in the range of 300 to 400°C. So the relative dielectric loss factor decreases in this the range. With the temperature increasing, the products which do not absorb microwave well. The rubber also keeps producing carbon black so that the ratio of carbon black increases. As a result, the relative loss factor increases. With air in container, the relative dielectric loss factor does not increase steadily. The relative dielectric loss factor indicates dissipation of microwave power. The relative dielectric loss factor is in direct proportion to ability of microwave absorption. The absorbing microwave ability of tire rubber increases with the increasing relative dielectric loss factor in the range of room temperature to 366°C.

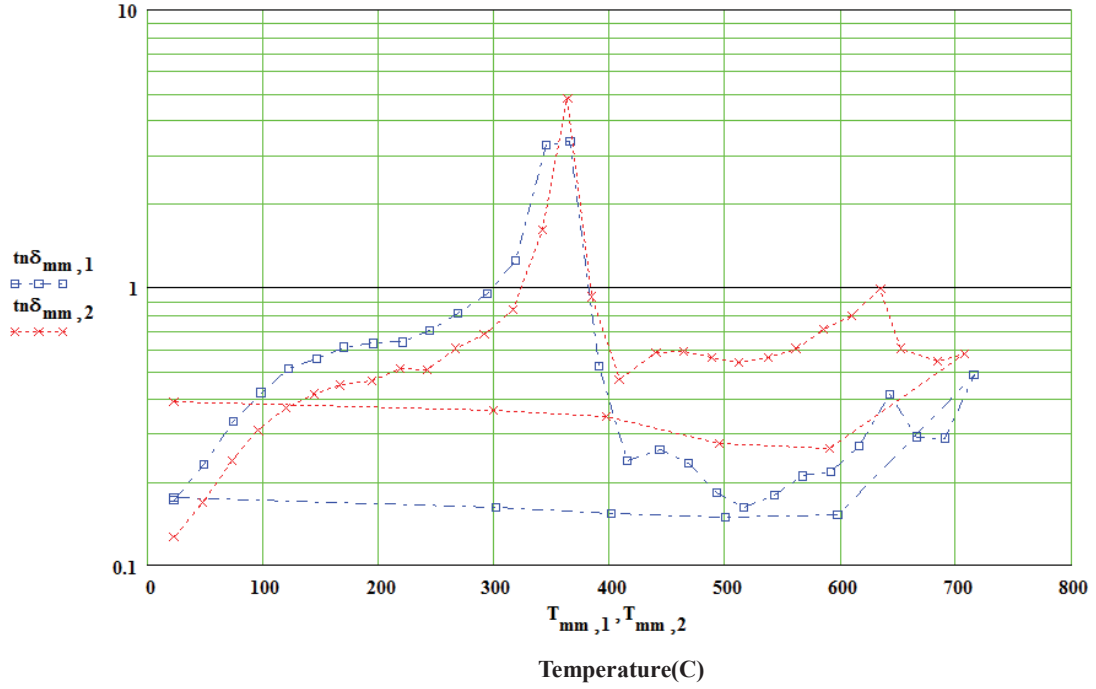


Figure 11. Temperature dependences of $\log(\tan\delta)$ under stagnant air. The $\tan\delta_{mm,1}$ is $\log(\tan\delta)$ at 915MHz, the $\tan\delta_{mm,2}$ is $\log(\tan\delta)$ at 2466MHz.

Figure 11 shows that the $\tan\delta$ of tire rubber at 915MHz keeps increasing in the range of room temperature to 366 °C. There is a substantial decrease in the range of 366 to 415°C. The $\tan\delta$ of tire rubber at 915MHz increases initially, and then it decreases in the range of 415 to 517°C. It increases firstly and it decreases after increasing in the range of 517 to 700°C. It increases from 700 to 800 °C. Finally, it keeps decreasing in the range of 800°C to room temperature and become stable at the end. The $\tan\delta$ of tire rubber at 2466MHz behaves similarly to the $\tan\delta$ of tire rubber at 915MHz. Only a difference is that the $\tan\delta$ of tier rubber at 2466MHz keeps increasing in the range of 600°C to room temperature. The $\tan\delta$ of tier rubber at 915MHz is higher than the $\tan\delta$ of tire rubber at 2466MHz in the range of room temperature to 345°C. Nevertheless, the $\tan\delta$ of tire rubber at 2466MHz is higher than

the $\tan\delta$ of tire rubber at 915MHz when temperature is up to 345°C.

Figure 11 shows the $\tan\delta$ is relatively independent of microwave frequency during pyrolysis. The differences between two different microwave frequencies are obvious when $\tan\delta$ is decreased.

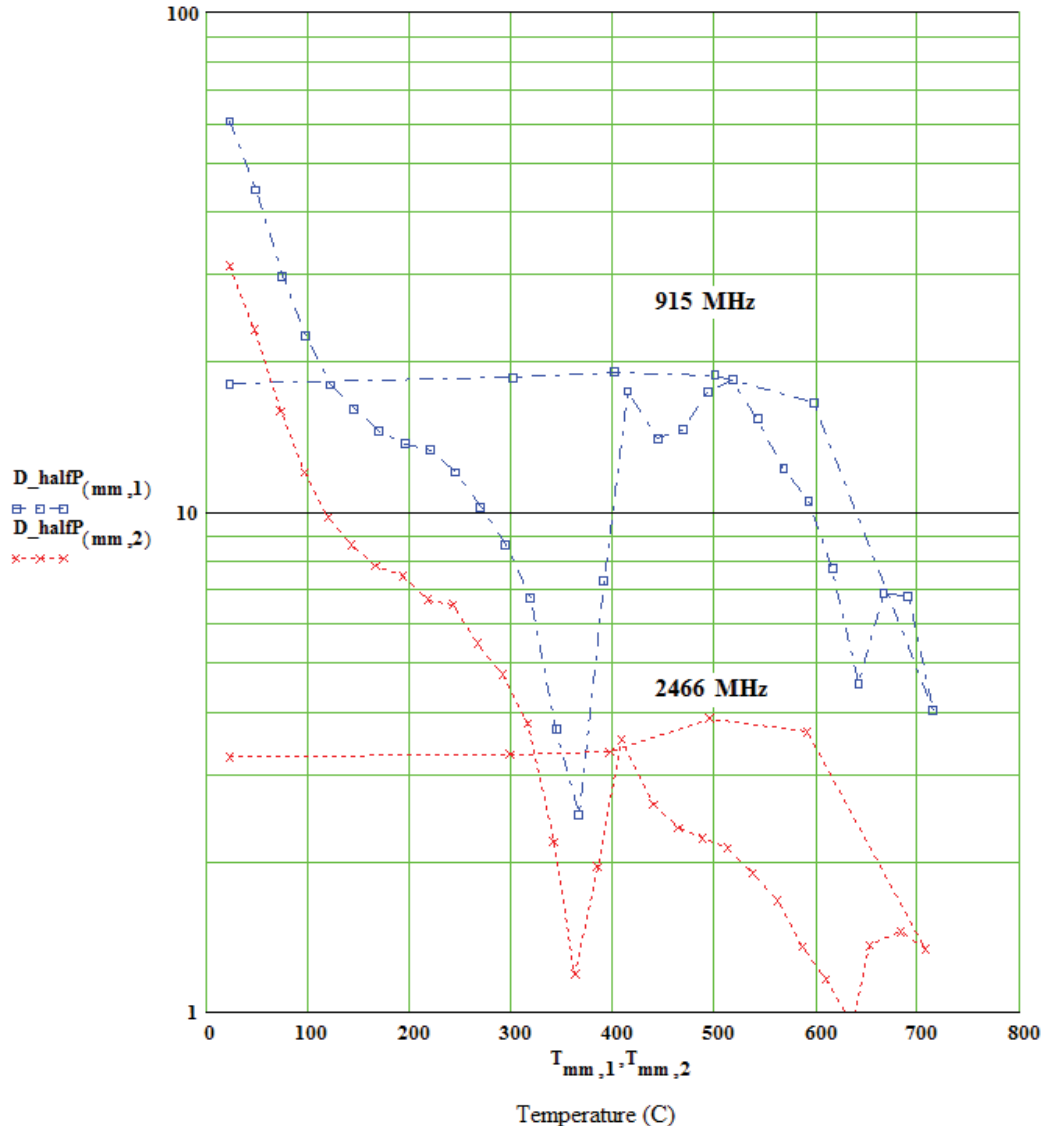


Figure 12. Temperature dependences of log(half-power depth) under stagnant air. The $D_{\text{halfP}}(\text{mm},1)$ is log(half-power depth) at 915MHz, the $D_{\text{halfP}}(\text{mm},2)$ is log(half-power depth) at 2466MHz.

Figure 12 shows that the half-power depth of tire rubber at 915MHz keeps decreasing in the range of room temperature to 366°C. Then it keeps increasing in the range of 366 to 415°C. It decreases in the range of 415 to 444°C. However it increases when temperature is increased to 444°C until there is a substantial decrease in the range of 500 to 642°C. The half-power depth of tire rubber at 915MHz increases firstly and decreases in the range of 642 to 666°C. The half-power depth of tire rubber at 2466MHz behaves similarly to the half-power depth of tire rubber at 915MHz from room temperature to 415°C and from 666 to 800°C. The difference is that the half-power depth of tire rubber 2466MHz keeps decreasing in the range of 415 to 642°C. The half-power depth of tire rubber at 915MHz is higher than the half-power depth of tire rubber at 2466MHz.

The half-power depth is inversely proportional to the microwave absorption capability.

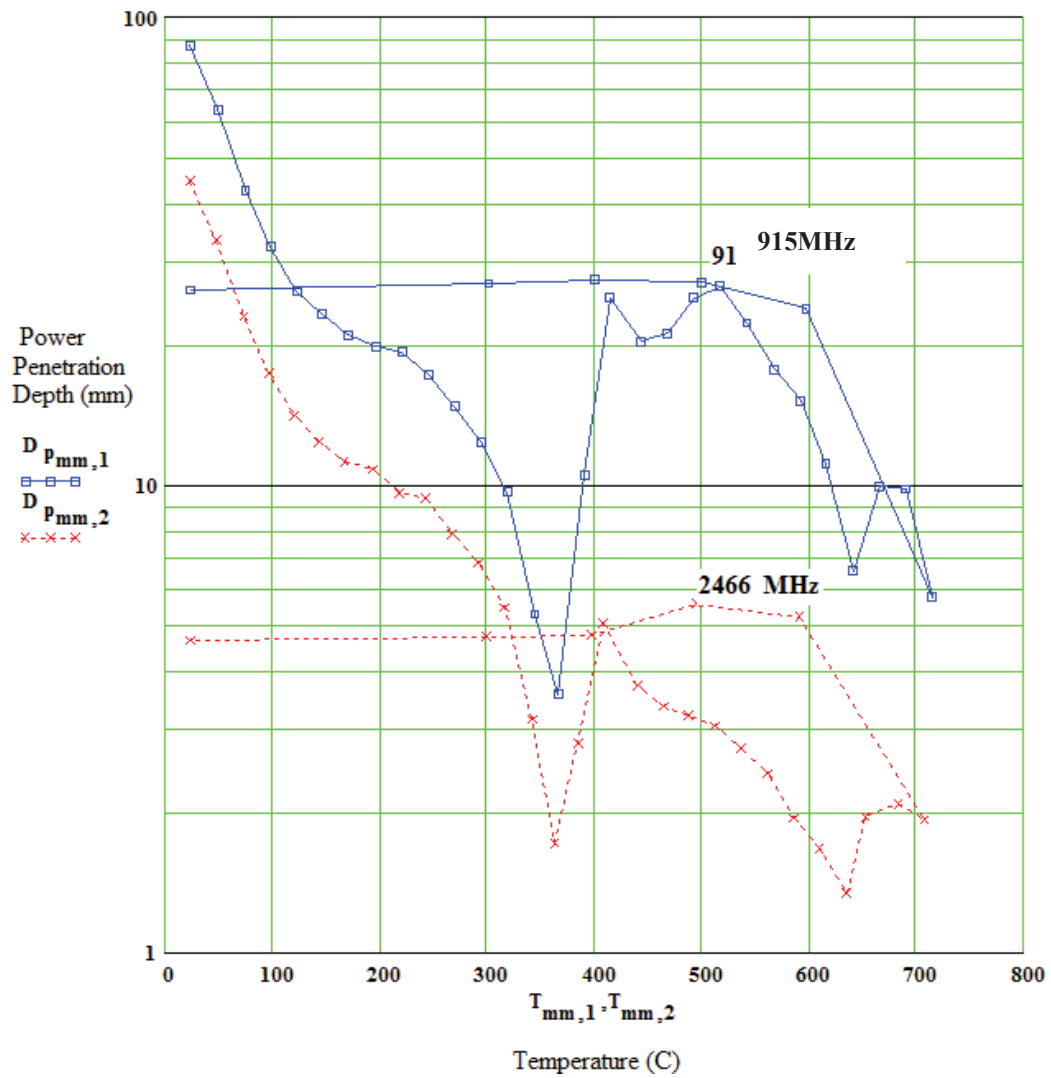


Figure 13. Temperature dependences of log(penetration depth) under stagnant air. The $D_{pmm,1}$ is log(penetration depth) at 915MHz, the $D_{pmm,2}$ is log(penetration depth) at 2466MHz.

Figure 13 shows that the penetration depth of tire rubber at 915MHz keeps decreasing in the range from room temperature to 366°C. It keeps increasing in the range of 366 to 415°C before it decreases in the range of 415 to 444°C. However, it increases when the temperature is increased to 444°C until there is a substantial

decrease in the range 500 to 642°C. It increases firstly and then decreases after increasing in the range of 642 to 666°C. The penetration depth of tire rubber at 2466MHz behaves similarly to the tire rubber at 915MHz from room temperature to 666°C. Only a difference is that the penetration depth of tire rubber at 2466MHz keeps decreasing in the range of 415 to 642°C. The penetration depth of tire rubber at 915MHz is higher than that at 2466MHz.

The penetration depth is inversely proportional to the microwave absorption capability. Tire rubber absorbs less microwave power when penetration depth increases. The increasing of $\tan\delta$ causes half-power depth decreasing in the range from room temperature to 366°C. There are some phase transformations during the tire rubber pyrolysis, making the ratio of carbon black decrease in the range of 366 to 415°C. So the ability of absorbing microwave is weakening and there is a substantial decrease in the plot. The variation of penetration depth is not stable when temperature is increased to 415°C resulting from reaction between air and carbon. Finally, with increasing temperature, the ratio of carbon black increases, leading to a reduction in the penetration depth.

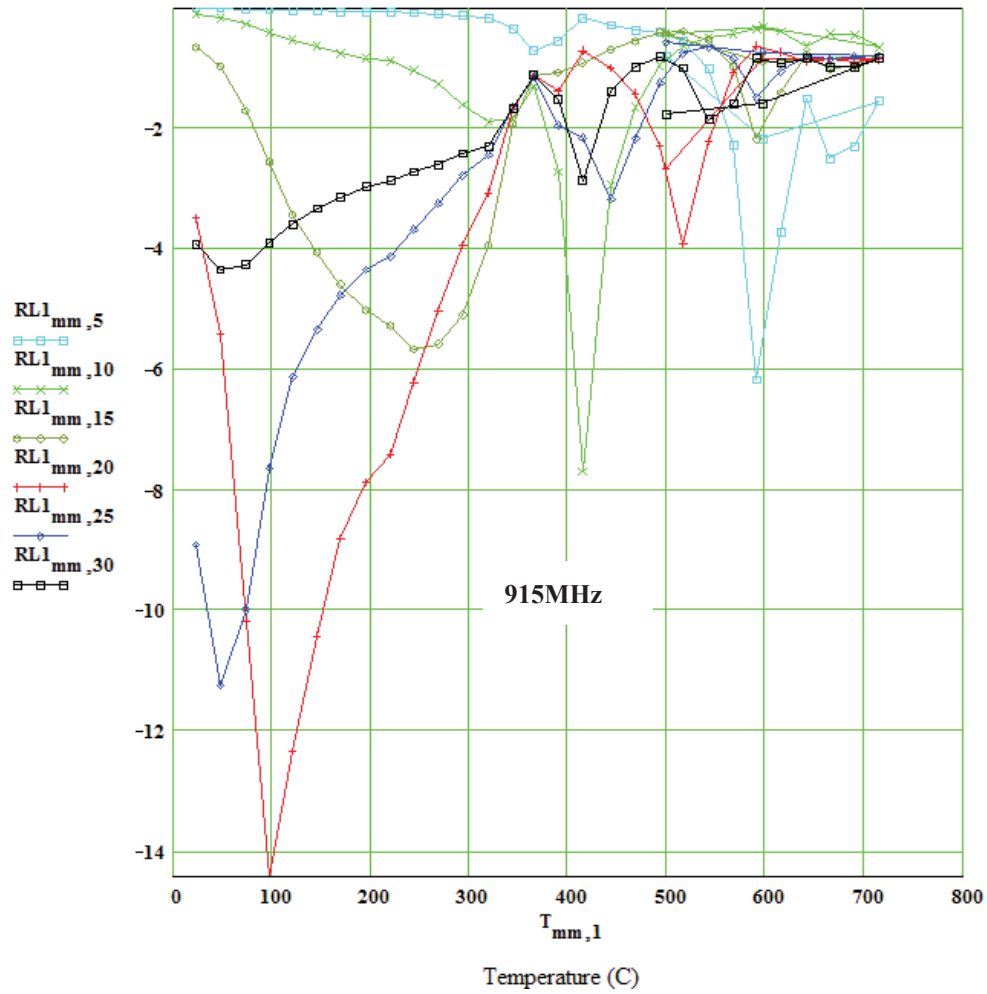


Figure 14. Temperature dependences of the reflection loss(dB) at 915MHz under stagnant air. The $RL_{mm,5}$ is the reflection loss of 5mm thick sample at 915MHz.

The $RL_{mm,10}$ is the reflection loss of 10mm thick sample at 915MHz. The $RL_{mm,15}$ is the reflection loss of 15mm thick sample at 915MHz. The $RL_{mm,20}$ is the reflection loss of 20mm thick sample at 915MHz. The $RL_{mm,25}$ is the reflection loss of 25mm thick sample at 915MHz. The $RL_{mm,30}$ is the reflection loss of 30mm thick sample at 915MHz.

Figure 14 shows that the reflection loss depends on temperature. Higher reflection loss means the sample has stronger ability to absorb microwave. There is a maximum absorption peak of 20mm thickness at 100°C. With the increasing of thickness of sample, the maximum absorption peak of same thickness shifts to lower temperature. With decreasing sample thickness the maximum absorption peak shifts to higher temperature. The temperature of maximum absorption intensity peak position is changing with the sample thickness. The temperature of maximum absorption intensity peak position is inversely proportional to the thickness of sample. The maximum absorption peak intensities of different thicknesses are not increasing with the higher thickness in the range of 5 to 20mm. So the peak intensity is determined by dielectric properties rather than the dimension of sample in 5 to 20mm. However, the intensity of maximum absorption peak is in inversely proportional to the thickness in the range of 20 to 30mm. So the peak intensity is determined by sample dimension in the range of 20 to 30mm. Moreover, the maximum absorption peak is at 100°C with the thickness which is 20mm. A further increase in thickness causes decrease of peak intensity.

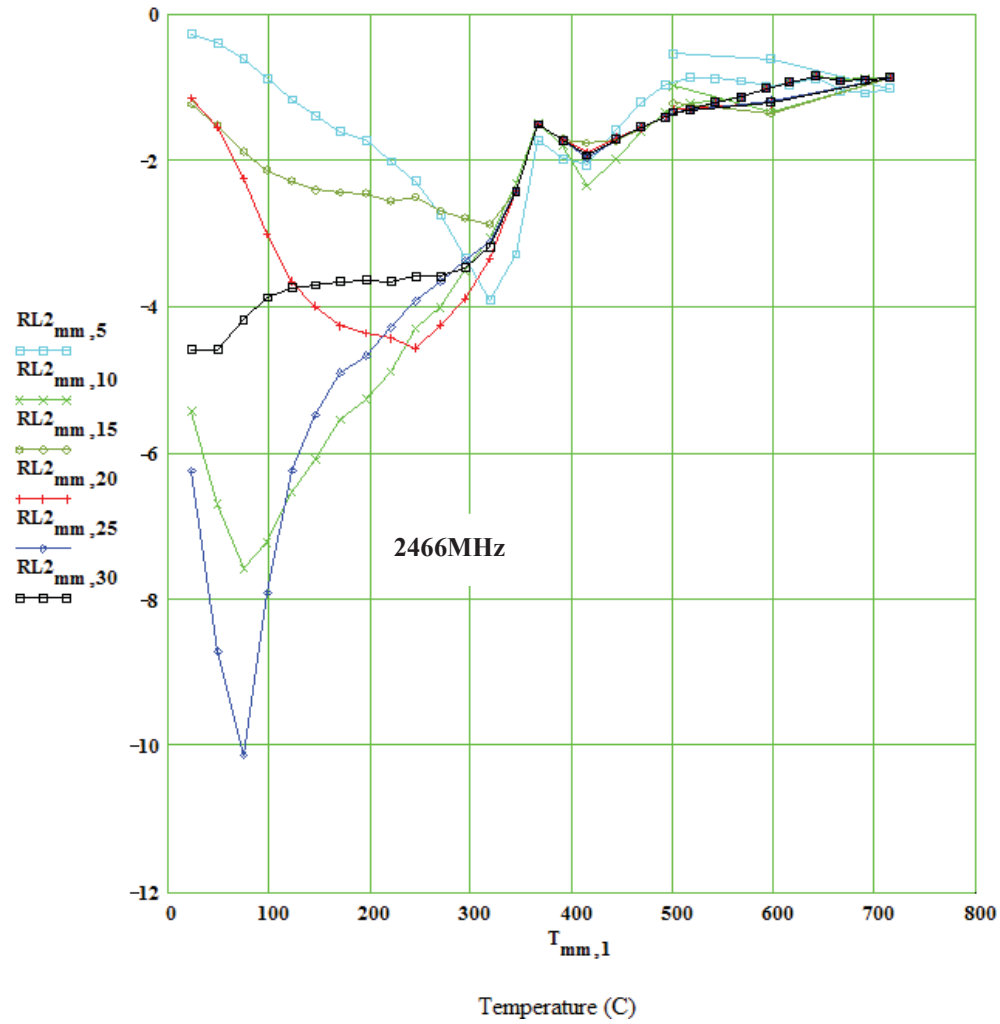


Figure 15. Temperature dependences of the reflection loss(dB) at 2466MHz under stagnant air. The $RL2_{mm,5}$ is the reflection loss of 5mm thick sample at 2466MHz. The $RL2_{mm,10}$ is the reflection loss of 10mm thick sample at 2466MHz. The $RL2_{mm,15}$ is the reflection loss of 15mm thick sample at 2466MHz. The $RL2_{mm,20}$ is the reflection loss of 20mm thick sample at 2466MHz. The $RL2_{mm,25}$ is the reflection loss of 25mmthick sample at 2466MHz. The $RL2_{mm,30}$ is the reflection loss of 30mm thick sample at 2466MHz.

Figure 15 shows that the reflection loss depends on temperature. The lower reflection loss means the sample has stronger microwave absorption. The reflection loss of tire rubber at 2466MHz has maximum absorption peak intensity in the range from room temperature to 100°C of 25mm. The maximum absorption peak intensity at 915MHz is higher than that at 2466MHz. But the thickness of the maximum absorption intensity of 915MHz is smaller than the maximum absorption intensity of 2466MHz. This difference is caused by the different dielectric loss factor of tire rubber at 915 and 2450MHz and different wavelengths corresponding to these two frequencies.

3.2 Experiment in nitrogen:

Done using a long holder (~ 500mm), pressurized to ~ 20 psig nitrogen:

The initial sample parameters were:

- a) Diameter: 3.50 ± 0.15 mm
- b) Length: 12.13 ± 0.05 mm
- c) Mass: 0.126 ± 0.002 gm
- d) Room temperature density: 1.08 ± 0.07 gm/cc.

The final sample parameters were:

- a) Diameter: 3.95 ± 0.25 mm
- b) Length: 20 ± 0.15 mm
- c) Mass: 0.056 ± 0.002 gm
- d) Room temperature density: 0.25 ± 0.08 gm/cc.

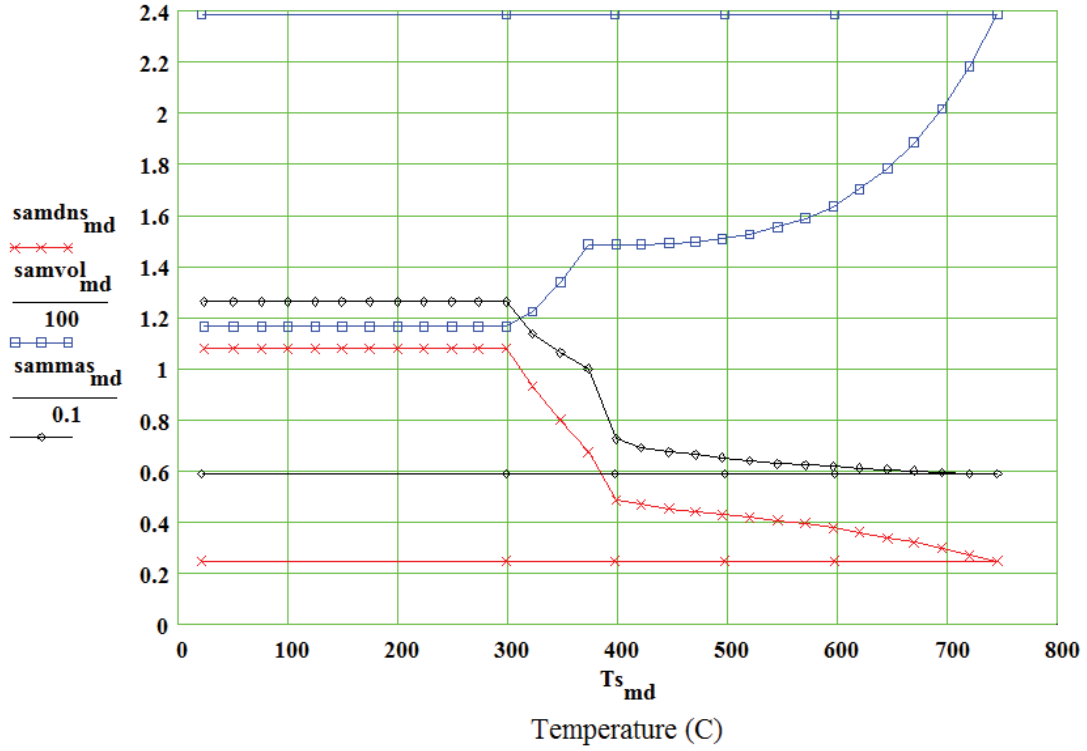


Figure 16. Temperature dependences of sample density(gm/cc), sample volume(mm³) and sample mass(gm) under UHP nitrogen. The samdns_{md} is sample density, the samvol_{md} is sample volume and the sammas_{md} is sample mass.

Figure 16 shows that the sample density is stable in the range of room temperature to 300°C. It keeps decreasing in the range of 300 to 800°C. The sample volume is stable in the range of room temperature to 300°C. Then it keeps increasing in the range of 300 to 800°C. The sample mass behaves similarly to the sample density.

During experiment, the holder is moved up by evolving gases which is produced during pyrolysis and the holder is raised up to 140mm high. This condition can increase the effective size of the sample, starting at 300°C. This condition may be

caused by the liquids which are produced by the tire rubber because this liquid eventually evaporated then the steam raise the holder with the vapor pressure. Finally leaving a “carbon” rod (the final sample) and a carbon coating on the holder walls above 675°C. This is the reason for the substantial increase of the sample mass under nitrogen which is different from the sample mass under stagnant air in the range of 400 to 700°C.

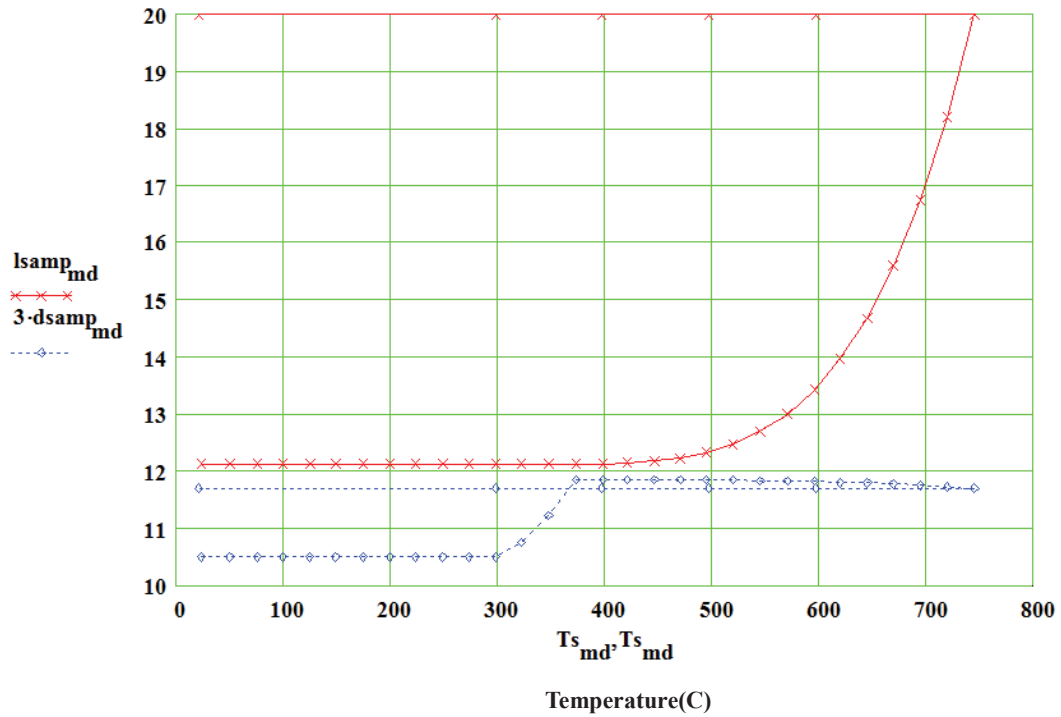


Figure 17. Temperature dependences of sample length(mm) and sample diameter(mm) under UHP nitrogen. The $lsamp_{md}$ is sample length and the $3-dsample_{md}$ is sample diameter.

Figure 17 shows that the sample length is stable in the range room temperature to 400°C. Then it keeps increasing in the range of 400 to 800°C. The sample diameter keeps stable in the range from room temperature to 300°C. Then it keeps increasing

in rang 300 to 375°C. It keeps decreasing slowly in the range 375 to 800°C.

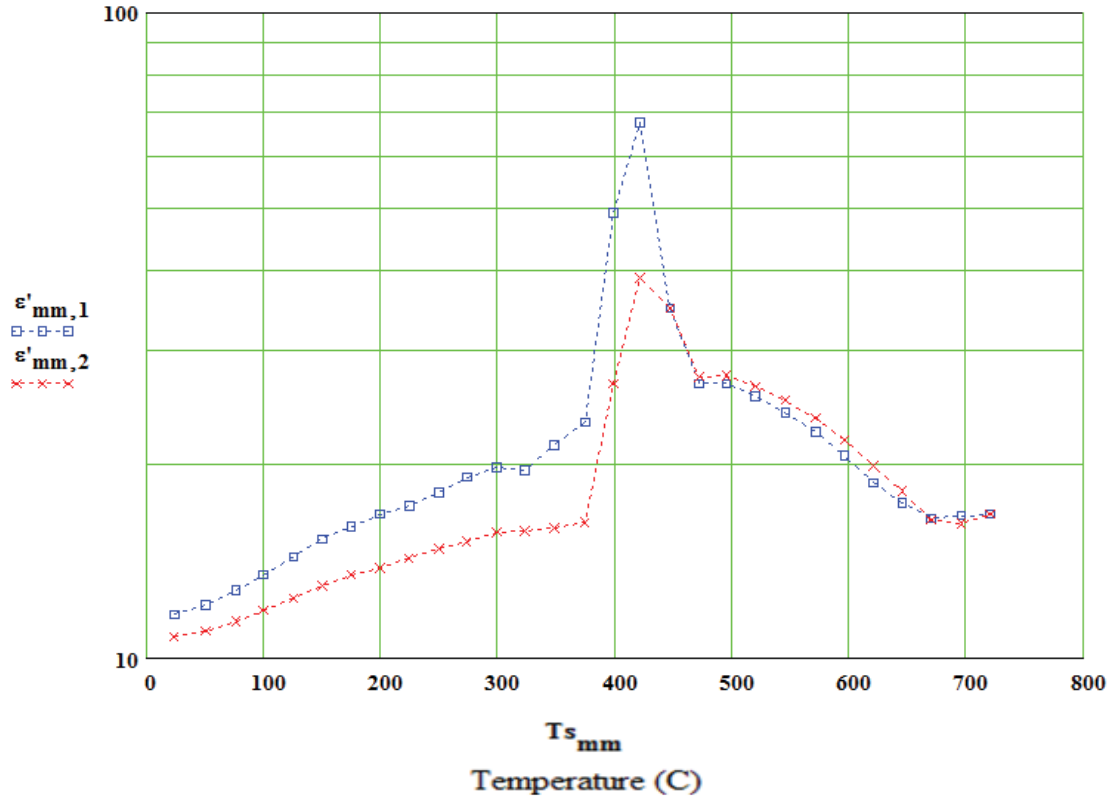


Figure 18. Temperature dependences of log(relative dielectric constant) under UHP nitrogen. The $\epsilon'_{mm,1}$ is the log(relative dielectric constant) at 915MHz, the $\epsilon'_{mm,2}$ is the log(relative dielectric constant) at 2466MHz.

Figure 18 shows the relative dielectric constant of tire rubber at 915MHz versus temperature. It increases slowly in the range of room temperature to 370°C. There is a substantial increase in the range of 370 to 412°C. It is the maximum dielectric constant is 412°C. A substantial decrease in the constant is found and it decreases slowly in the range of 412 to 466°C. The relative dielectric constant of tire rubber at 2466MHz increases slowly in the range of room temperature to 367°C. There is a substantial increase in the range of 367 to 409°C and the highest constant is found at 409°C. There is a substantial decrease in the range of 409 to 457°C. The relative

dielectric constant of tire rubber at 915MHz is higher than the relative dielectric constant of tire rubber at 2466MHz in from room temperature to 450°C. The relative dielectric constant of tire rubber at 915MHz is lower than the relative dielectric constant of tire rubber at 2466MHz when temperature is decreased to 450°C.

Figure 18 shows that the relative dielectric constant under UHP nitrogen is relatively independent of the microwave frequency in the range from room temperature to 370°C and from 457 to 800°C. But the relative dielectric constant under UHP nitrogen is dependent on the microwave frequency in the range of 370°C and 457°C. The dielectric constant peak indicates a phase transformation in the range of 370 to 457°C. The condition under UHP nitrogen is different from the one under stagnant air. Because nitrogen is protection gas for this experiment, nitrogen will not react with the sample so the ratio of carbon will increase faster than under stagnant air.

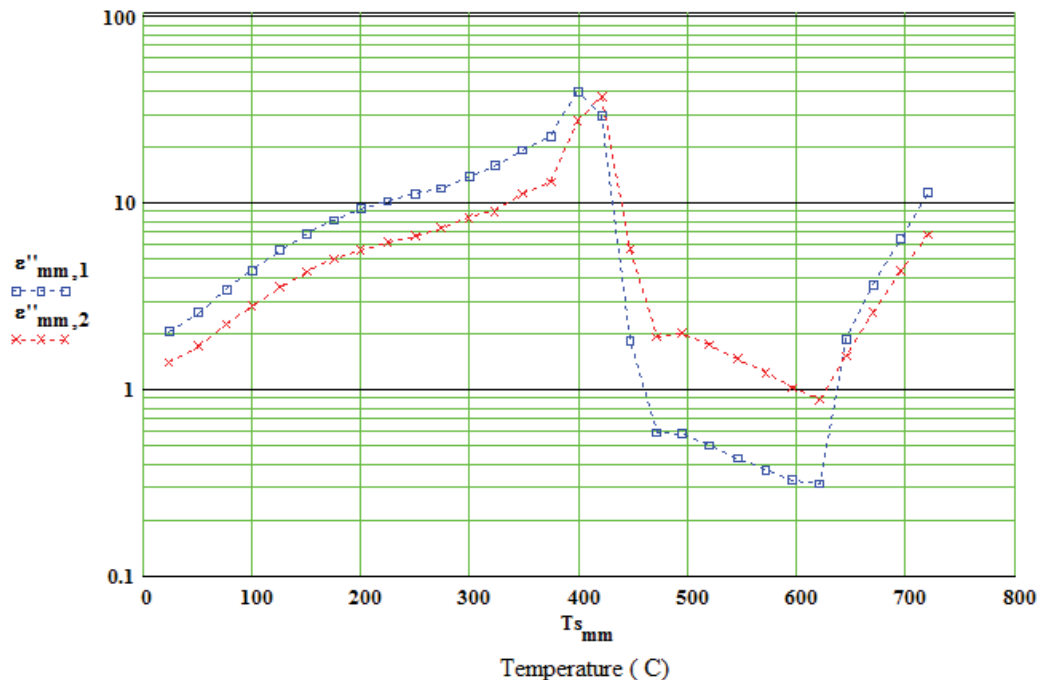


Figure 19. Temperature dependences of log(relative dielectric loss factor) under

UHP nitrogen. The $\varepsilon''_{mm,1}$ is the log(relative dielectric loss factor) at 915MHz, the $\varepsilon''_{mm,2}$ the log(relative dielectric loss factor) at 2466MHz.

Figure 19 shows that the variation of relative dielectric loss factor of tire rubber with temperature at 915MHz can be separated into three distinct stages. It keeps increasing in the range of room temperature to 400°C. There is a substantial decrease in the range of 400 to 500°C. The relative dielectric loss factor of tire rubber at 915MHz keeps decreasing until the temperature goes up to 600°C. Finally, there is a substantial increase in the range of 600 to 800°C. The relative dielectric loss factor of tire rubber at 2466MHz behaves similarly to relative dielectric loss factor of tire rubber at 915MHz. Then the relative dielectric loss factor of tire rubber at 915MHz is higher than the relative dielectric loss factor of tire rubber at 2466MHz in the range from 400 to 650°C. The relative dielectric loss factor of tire rubber at 915MHz is higher than the relative dielectric loss factor of tire rubber at 2466MHz in the range of 650 to 800°C.

Figure 19 shows that data of the relative dielectric loss factor of tire rubber at 915MHz isn't higher than the data of relative dielectric loss factor of tire rubber at 2466MHz all the time during temperature increasing so the relative dielectric loss factor does not fit the equation $\varepsilon'' = \frac{1}{2\pi f \varepsilon_0 R(\frac{\pi D^2}{4L})}$. As a result, the microwave loss mechanism for pyrolyzed tire rubber is not pure free electron conduction. With increasing temperature, the increasing content of carbon black causes the increasing of relative dielectric loss factor. However, little air in the container can react with carbon black. And there is an obvious dielectric loss peak in the range of 400 to 500°C. This is a typical interfacial/relaxation polarization phenomena behavior, usually indicating a change in the material associated with the loss of an insulating barrier [22]. It indicates a phase transformation and the product do not absorb

microwave well in the range of 400 to 500°C. With the temperature increasing, the products which do not absorb microwave well are pyrolyzed and the rubber also keeps producing carbon black so that the content of carbon black increases. As a result, the relative loss factor increases. But with air in container relative dielectric loss factor isn't increase steadily. The relative dielectric loss factor indicates loss of microwave power. And the relative dielectric loss factor is in direct proportion to ability of absorbing microwave. In the range of room temperature to 400°C, the microwave absorbing ability of tire rubber is increasing with the increasing of relative dielectric loss factor. But the substantial decrease is different with the data under stagnant air.

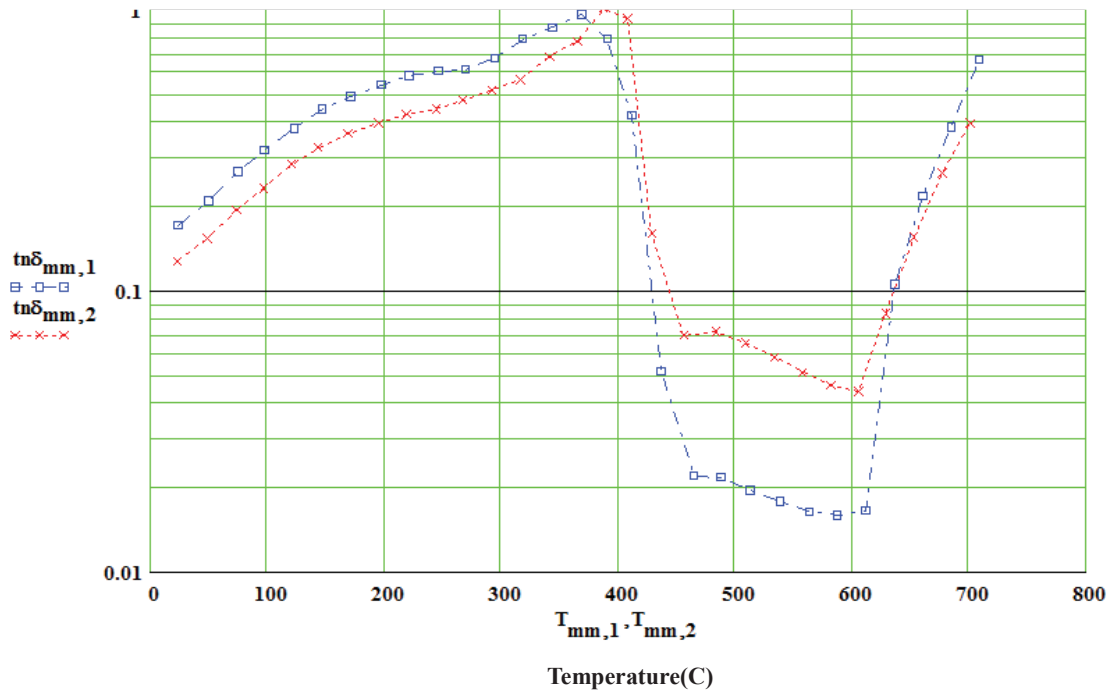


Figure 20. Temperature dependences of $\log(\tan\delta)$ under UHP nitrogen. The $\tan\delta_{\text{mm},1}$ is $\log(\tan\delta)$ at 915MHz, the $\tan\delta_{\text{mm},2}$ is $\log(\tan\delta)$ at 2466MHz.

Figure 20 shows that the variation of $\tan\delta$ of tire rubber at 915MHz can be

separate into four distinct stages. The $\tan\delta$ of tire rubber at 915MHz keeps increasing in the range of room temperature to 370°C. There is a substantial decrease in the range of 370 to 466°C. Then it decreases lowly until there is a substantial increase in the tangent from 612 to 800°C. The $\tan\delta$ of tire rubber at 2466MHz behaves similarly to that at 915MHz. The $\tan\delta$ of tire rubber at 915MHz is larger than the $\tan\delta$ of tire rubber at 2466MHz in the range of room temperature to 370°C. The $\tan\delta$ of tire rubber at 2466MHz is higher than the $\tan\delta$ of tire rubber at 915MHz in the range of 370 to 612°C. However, the $\tan\delta$ of tire rubber at 2466MHz is smaller than the $\tan\delta$ of tire rubber at 915MHz in the range of 612 to 800 °C.

Figure 20 shows that the $\tan\delta$ increases with increasing $\frac{\epsilon''}{\epsilon'}$ in the range of room temperature to 370°C. There is a substantial decrease in the $\tan\delta$ under stagnant air from 370 to 500°C.

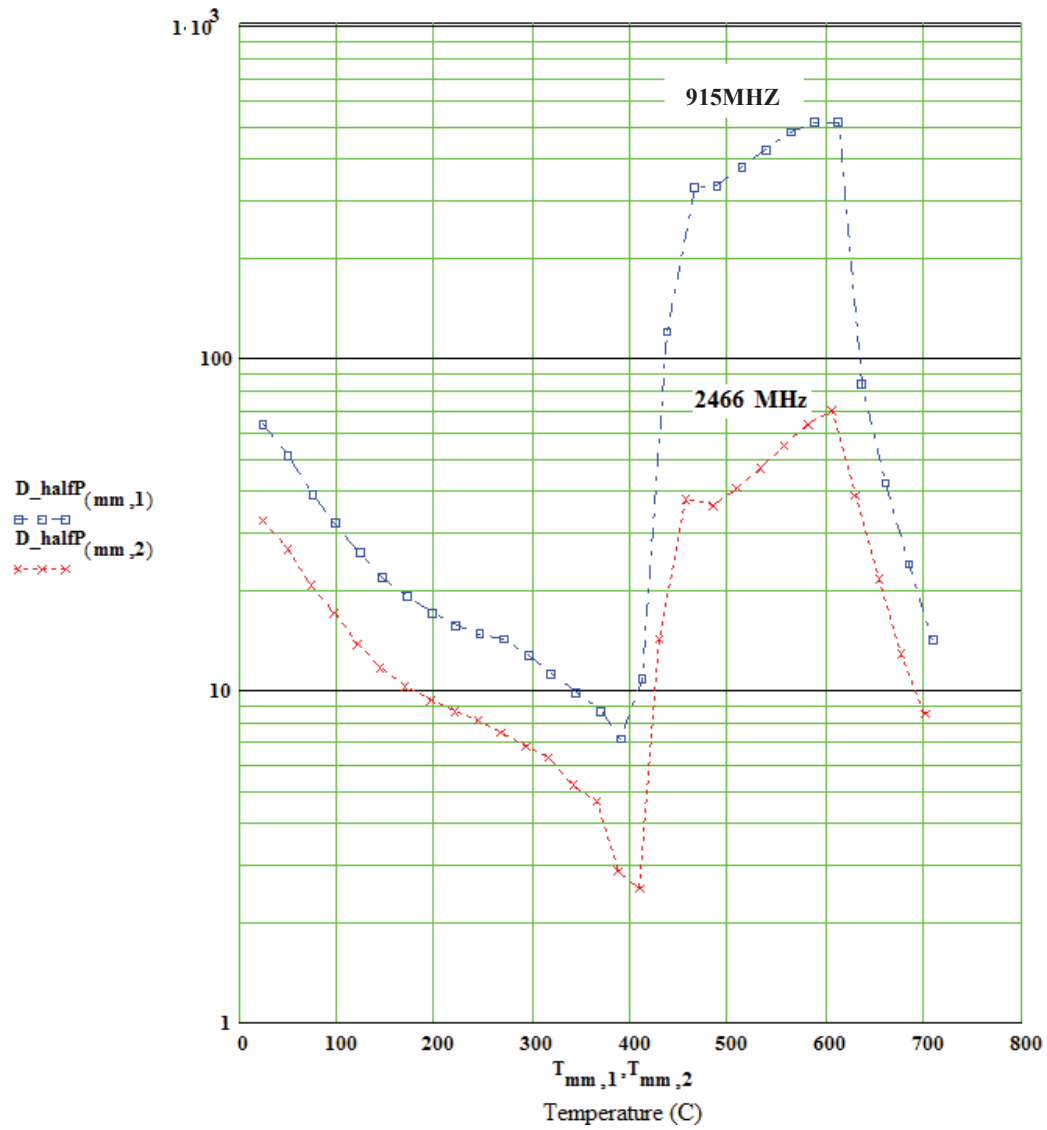


Figure 21. Temperature dependences of log(half-power depth) under UHP nitrogen. The $D_{\text{halfP}}(\text{mm},1)$ is log(half-power depth) at 915MHz, the $D_{\text{halfP}}(\text{mm},2)$ is log(half-power depth) at 2466MHz.

Figure 21 shows the variation of half-power depth of tire rubber with temperature at 915MHz. It keeps decreasing in the range of room temperature to 400°C. There is a substantial increase in the depth in the range of 400 to 500°C. Then

the half-power depth of tire rubber at 915MHz keeps increasing from 500 to 600°C. Finally, there is a substantial decrease in the range of 600 to 700°C. The half-power depth of tire rubber at 2466MHz behaves similarly to the half-power depth of tire rubber at 915MHz. The half-power depth of tire rubber at 915MHz is higher than that at 2466MHz.

The half-power depth is inversely proportional to the microwave absorbing properties.

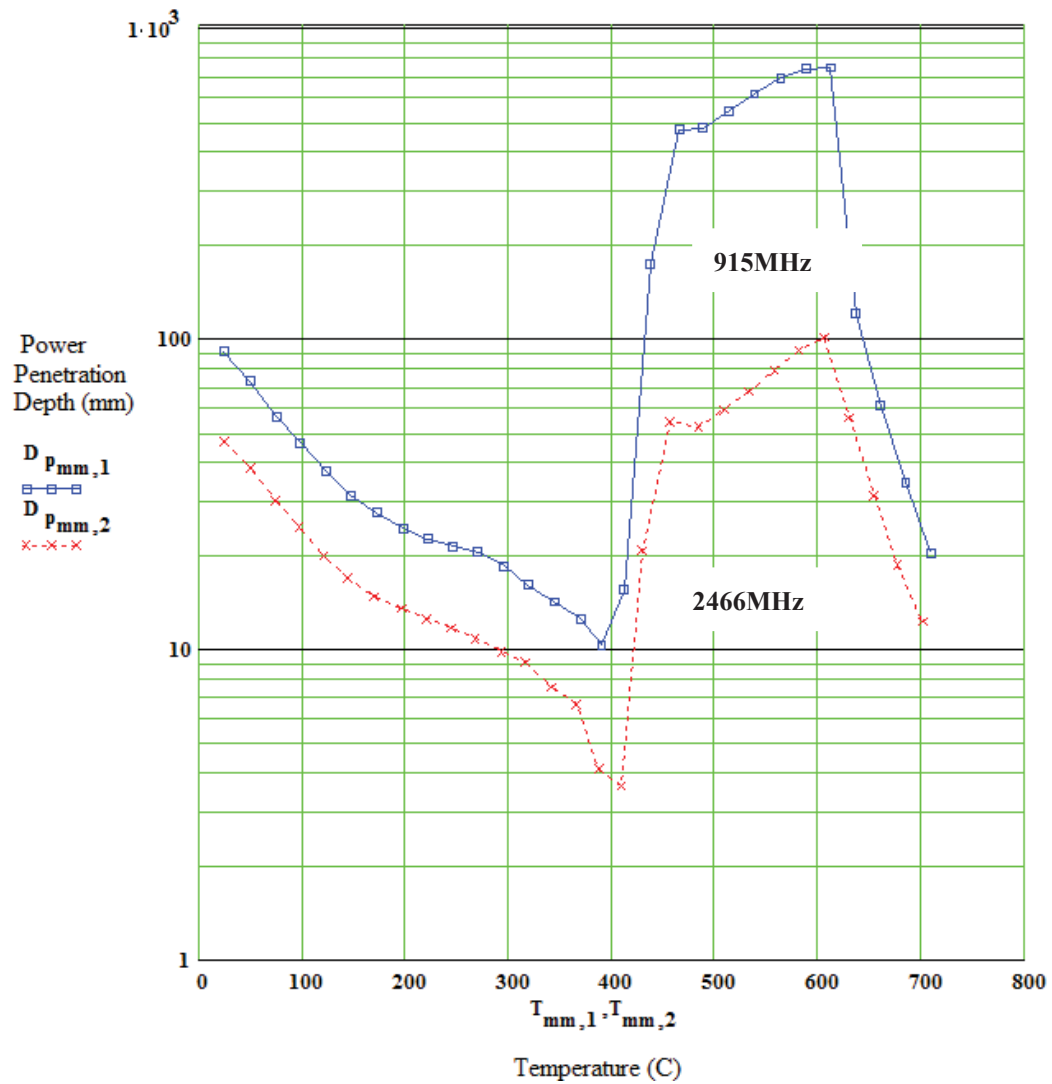


Figure 22. Temperature dependences of log(penetration Depth) under UHP nitrogen. The $D_{pmm,1}$ is log(penetration depth) at 915MHz, the $D_{pmm,2}$ is log(penetration depth) at 2466MHz.

Figure 22 shows that the penetration depth of tire rubber at 915MHz can be separated into four distinct stages. The penetration depth of tire rubber at 915MHz keeps decreasing in the range of room temperature to 400°C. There is a substantial increase of penetration depth in the range of 400 to 500°C. The penetration depth at 915MHz keeps increasing in the range of 500 to 600°C. Finally, there is a substantial decrease in the range of 600 to 700°C. The variation of penetration depth of tire rubber at 2466MHz behaves similarly to the penetration depth of tire rubber at 915MHz. The penetration depth of tire rubber at 915MHz is larger than that at 2466MHz.

The increasing of $\tan\delta$ causes half-power depth decreasing in the range of room temperature to 400°C. There are some phase transformations during the tire rubber pyrolysis, making the content of carbon black decreased in the range of 400 to 500°C. Hence, the ability of absorbing microwave decreases and there is a substantial decrease in the plot. The line of penetration depth under UHP nitrogen is more stable than the line of penetration depth under stagnant air at temperatures below 400°C, due to the protection of nitrogen gas.

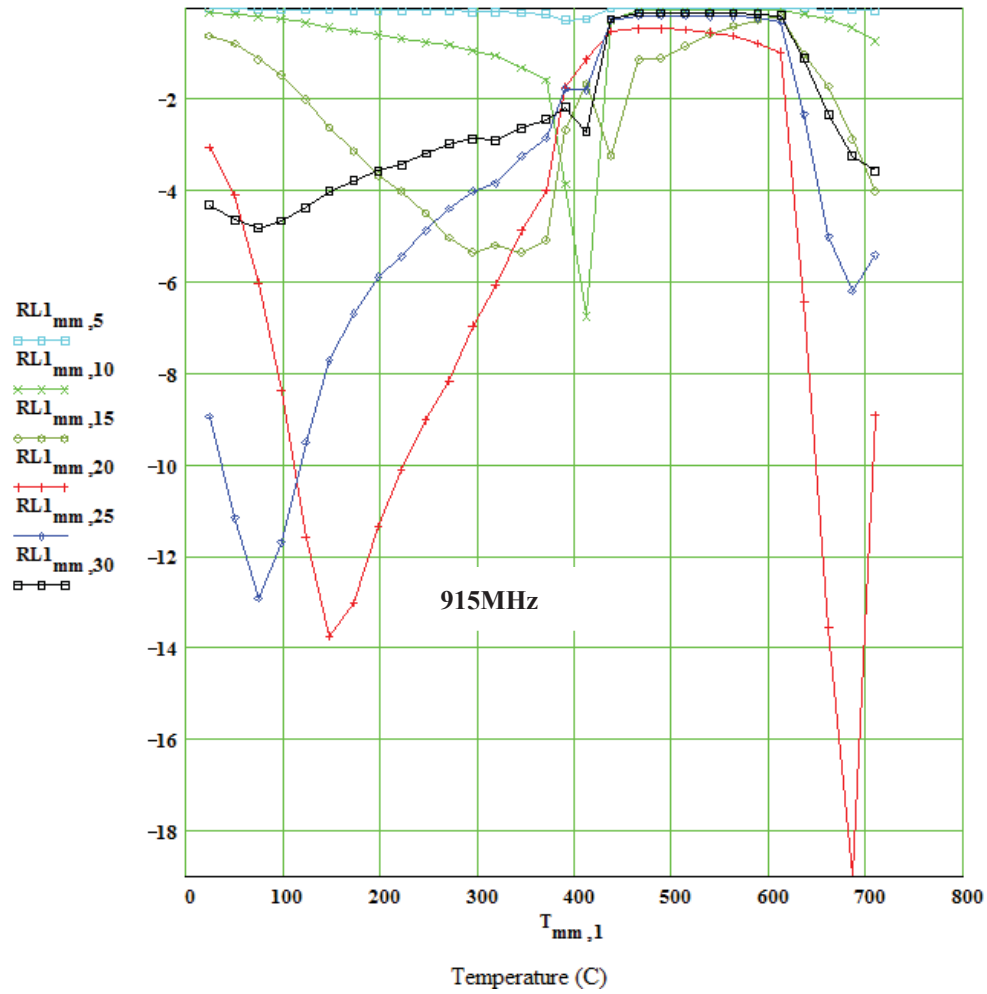


Figure 23. Temperature dependences of the reflection loss(dB) at 915MHz UHP nitrogen. The $RL_{mm,5}$ is the reflection loss of 5mm thick sample at 915MHz. The $RL_{mm,10}$ is the reflection loss of 10mm thick sample at 915MHz. The $RL_{mm,15}$ is the reflection loss of 15mm thick sample at 915MHz. The $RL_{mm,20}$ is the reflection loss of 20mm thick sample at 915MHz. The $RL_{mm,25}$ is the reflection loss of 25mm thick sample at 915MHz. The $RL_{mm,30}$ is the reflection loss of 30mm thick sample at 915MHz.

Figure 23 shows that the reflection loss depends on temperature. Higher reflection loss means the sample has stronger ability to absorb microwave. There is a maximum absorption peak of 20mm thickness at 100°C. With increasing thickness of sample, the maximum absorption peak of same thickness shifts to a lower temperature. The temperature of maximum absorption peak position is changing with the sample thickness. The maximum absorption peak intensities of different thicknesses do not increase with increasing thickness in the range of 5 to 20mm. So the peak intensity is determined by dielectric properties rather than the dimension of sample in 5mm to 20mm. However the intensity of the maximum absorption peak is inversely proportional to the thickness in the range from 20 to 30mm. So the peak intensity is determined by sample dimension in the range of 20mm to 30mm. Moreover, the maximum absorption peak is in the range of 600 to 700°C of 20mm.

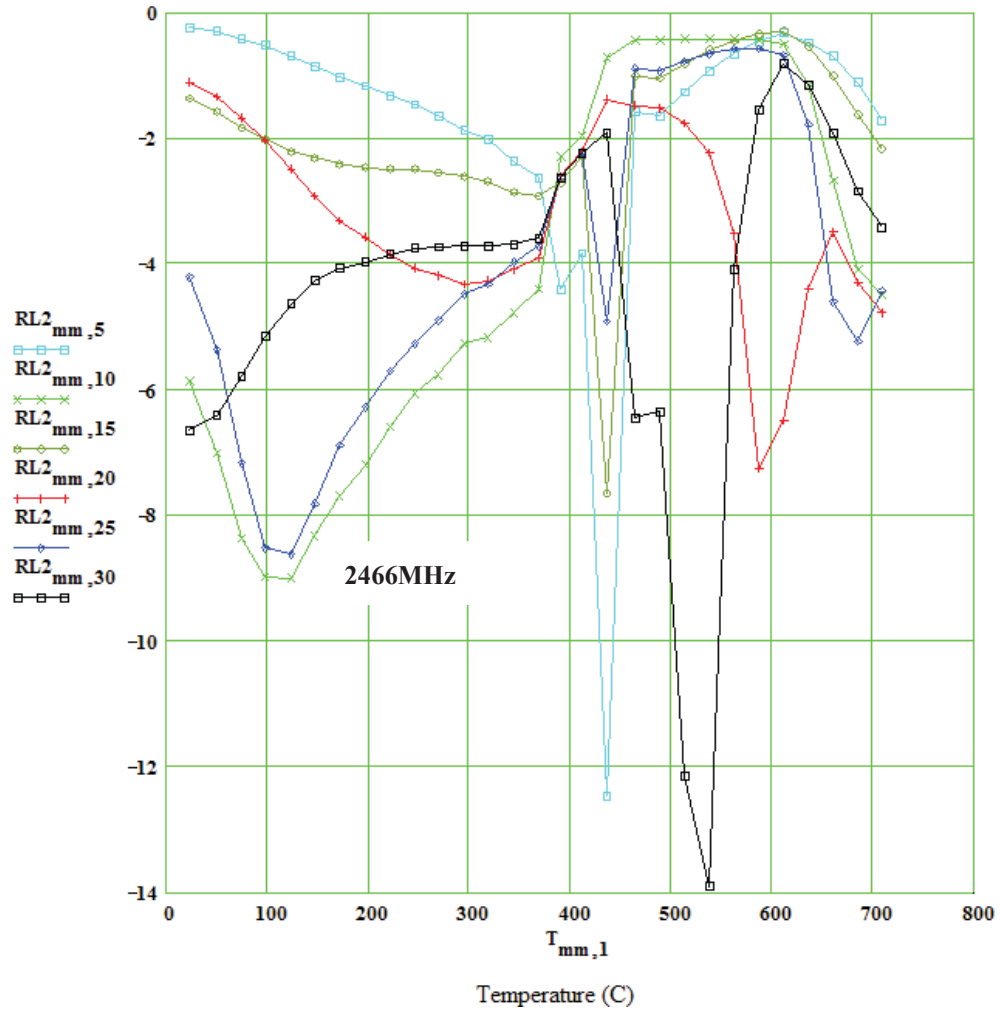


Figure 24. Temperature dependences of the reflection loss(dB) at 2466MHz under UHP nitrogen. The RL2_{mm,5} is the reflection loss of 5mm thick sample at 2466MHz. The RL2_{mm,10} is the reflection loss of 10mm thick sample at 2466MHz. The RL2_{mm,15} is the reflection loss of 15mm thinness sample at 2466MHz. The RL2_{mm,20} is the reflection loss of 20mm thick sample at 2466MHz. The RL2_{mm,25} is the reflection loss of 25mm thick sample at 2466MHz. The RL2_{mm,30} is the reflection loss of 30mm thick sample at 2466MHz.

Figure 24 shows that the reflection loss depends on temperature. Higher the reflection loss means the sample has stronger ability of absorbing microwave. The variation of reflection loss presents the maximum absorption peak intensity in the range of 500 to 600°C when the sample has a thickness of 30mm. The maximum absorption intensity of 915MHz is higher than the maximum absorption intensity of 2466MHz. But the thickness of the maximum absorption peak intensity of 915MHz is smaller than the maximum absorption intensity of 2466MHz. This is resulted from the difference between the dielectric loss factor of tire rubber at 915MHz and 2450MHz and that between wavelengths corresponding to these two frequencies. The maximum absorption peak intensity at 2466MHz is in the range of 500 to 600°C for the sample having a thickness of 30mm. But the maximum absorption intensity of 2466MHz under stagnant air is in the range of room temperature to 100°C of 25mm.

Conclusion:

The dielectric properties of the tire rubber from the Cooper Company were measured at 915 and 2466MHz under stagnant air and UHP nitrogen from room temperature to 800°C. The physical properties (density, volume, mass, length, diameter) of the tire rubber remain stable at low temperatures under stagnant air and under UHP nitrogen. However, there are increases in volume of the tire rubber under stagnant air and UHP nitrogen. And there are decreases in all physical properties of the tire rubber, such as the density, mass and length. These changes are due to the solid phase of tire rubber transform to liquid and gas phase with the increasing of temperature and release of volatiles. The relative dielectric properties remain relatively steady in the range of room temperature to 400°C under stagnant air. The relative dielectric loss factor is not stable and the relative dielectric constant keeps increasing in the range of 400 to 800°C under stagnant air. This phenomenon is due to the phase transformation and release of volatiles. The dielectric properties of tire rubber under UHP nitrogen keep increasing from room temperature to 300°C. During experiment the sample holder is moved up by evolving gases which is produced during pyrolysis and the holder is raised up to 140mm high. This condition can increase the effective size of the sample, starting at 300°C. This condition should be caused by the liquids which is produced by sample and this liquid eventually pyrolyzed, leaving a “carbon” rod (the final sample) and a carbon coating on the holder walls above 675°C. Nitrogen is protection gas which will not react with tire rubber. It makes the dielectric properties, half-power depth, penetration depth and physical properties of tire rubber under UHP nitrogen have more sharp increases and decreases than the counterparts of tire rubber under stagnant air in the range of 300 to 800°C. The calculations of half-power depths and penetration depths of tire rubber under stagnant air and UHP nitrogen confirm that the pyrolysis process considerably

improves microwave absorption capability of the tire rubber at high temperature (300 to 500°C). The calculations of reflection loss of tire rubber under stagnant air and under UHP nitrogen shows that the maximum reflection loss occurs at 915MHz when the sample has a thickness of 20 mm. The tire rubber dimension has a substantial impact on the overall microwave absorption of the tire rubber during pyrolysis and thus on the efficiency of microwave tire rubber pyrolysis.

References

- [1] Martinez, David F., *United States Patent*, US5304576 A (1994), “Soaking in a solvent to reduce tensile strength, applying shear force to disintegrate rubber from reinforcement; sorting”.
- [2] Yi Fang, Maosheng Zhan*, Ying Wang, *Materials & Design*, 22 (2001) 123-127, “The status of recycling of waste rubber”.
- [3] LiuH., Mead J., Stacer R., *Chelsea Center For Recycling And Economic Development*, (1998), “Environmental Impacts of Recycling Rubber in Light Fill Applications: Summary & Evaluation Of Existing Literature University of Massachusetts”.
- [4] Price, Willard, and Edgar D. Smith., *International Journal of Environmental Technology and Management* (2006)6.3-4, 363-364, “Waste tire recycling: environmental benefits and commercial challenges”.
- [5] R.C Walter, K.C Bass, W.E Roseveare, *Ind. Eng. Chem.*, 48 (1978)138–143, “Degradation of rayon tyres at elevated temperature”.
- [6] Shang J, Mei J, Notestein J., *USA: Department of Energy*, (1981) No. DOE/METC-8614068, “Fluidized-bed combustion of scrap tyres, technical notes from Annual Report”.
- [7] L Berti, M Marani, R Scialdoni, *RisparmioEnergetico*, 29 (1990), 23–32, “Valutazione e misure delle emissioni di un impianto di combustione di pneumatici”.
- [8] Allott K., *Process Engg. Environmental Protection*, (1991) 45–46, “crapped tyres: their potential as a source of energy or raw materials”.
- [9] Coronidi M, Ranaldi E., *Relazione Finale*, (1995) vol. 1, FISIA/AMB-TEIN-G-004 248, “Prove di combustione granulato di pneumatici

nell'inceneritore a letto fluido ABI-2000”.

[10] Rausa R, Pollesel P., *J. Analytical and Applied Pyrolysis*, (1997) 40–41:369, “Pyrolysis of automotive shredded residue: influence of temperature on the distribution of products”.

[11] “Tire recycling”, last modified April 8, (2014),

http://en.wikipedia.org/wiki/Tire_recycling

[12] “pyrolysis”, last modified April 29, (2014),

<http://en.wikipedia.org/wiki/Pyrolysis>

[13] Kaminsky W, Sinn H., *Proc. ACS Symposium Series*, (1980), 130-423, “Pyrolysis of plastic waste and scrap tyres using a fluidized-bed process”.

[14] Roy C, Unsworth J., *London: Elsevier Applied Science*, (1989) 180–89, “Pyrolysis and gasification. In: Ferrero GL, Maniatis K, Buekens A, Bridgewater A, editors”.

[15] P.T William, S Besler, D.T Taylor, *Fuel*, 69 (1990) 1474–1482, “The pyrolysis of scrap automotive tyres”.

[16] P.T William, D.T Taylor, *Fuel*, 72 (1993) 1469–1474, “Aromatization of tyre pyrolysis oil to yield pyrolytic aromatic hydrocarbons”.

[17] Y Chang, *Resources Conservation Recycling*, 17 (1996) 125–139, “On the pyrolysis of waste tyres degradation rate products yields”.

[18] Fortuna F, Mincarini M, Cornacchia G, Sharma VK., *Analytical and Applied Pyrolysis*, (1997), 40–41, 403–417, “Pilot-scale experimental pyrolysis plant: mechanical and operational aspects”.

[19] Xiang Sun, Master thesis, Michigan Technology University, (2006), “Treatment of electric arc furnace dust by microwave heating”.

[20] Советская Энциклопедия, *Great Soviet Encyclopedia*, (1979), “Resistance furnace”.

[21] M. Al-Harabsheh, S.W. Kingman*, *Hydrometallurgy*, 73 (2004) 189-203,

“Microwave-assisted leaching-a review”.

[22] Zhiwei Peng, Jiann-Yang Hwang*, Byoung-Gon Kim, Joe Mouris, Ron Hutcheon, *Energy Fuels*, 26 (2012) 5146–5151, “Microwave Absorption Capability of High Volatile Bituminous Coal during Pyrolysis”.

[23] Zhiwei Peng, Jiann-Yang Hwang*, Matthew Andriese, *Ceramics International*, 39 (2013) 6721–6725, “Design of double-layer ceramic absorbers for microwave heating”.

[24] Guozhu Shen, Zheng Xu, Yi Li, *Journal of Magnetism and Magnetic Materials*, 301 (2006), 325–330, “Absorbing properties and structural design of microwave absorbers based on W-type La-doped ferrite and carbon fiber composites”.

[25] Zhiwei Peng, Jiann-Yang Hwang, Joe Mouris, Ron Hutcheon, Xiang Sun, *Metals & Materials Society and ASM International*, (2011) 2259-2263, “Microwave Absorption Characteristics of Conventionally Heated Nonstoichiometric Ferrous Oxide”.

[26] Guillermo San Miguel, Geoffrey D. Fowler, Christopher J. Sollars*, *Carbon* 41 (2003) 1009–1016, “A study of the characteristics of activated carbons produced by steam and carbon dioxide activation of waste tyre rubber”.

[27] Bendida Sahouli*, Silvia Blather, Francois Brouers, Hans Darmstadt, Christian Royt, Serge Kaliaguine, *Fuel*, 75 (1996) 1244-1250, “Surface morphology and chemistry of commercial carbon black and carbon black from vacuum pyrolysis of used tyres”.

[28] M.C. Bignozzi*, F. Sandrolini, *Cement and Concrete Research*, 36 (2006) 735–739, “Tyre rubber waste recycling in self-compacting concrete”.

[29] R. Helleur*, N. Popovic, M. Ikura, M. Stanciulescu, D. Liu, *Journal of Analytical and Applied Pyrolysis*, 58–59 (2001) 813–824, “Characterization and potential applications of pyrolytic char from ablative pyrolysis of used tires”.

- [30] V.K. Gupta*, Bina Gupta, ArshiRastogi, Shilpi Agarwal, Arunima Nayak, *Journal of Hazardous Materials*, 186 (2011) 891–901, “A comparative investigation on adsorption performances of mesoporous activated carbon prepared from waste rubber tire and activated carbon for hazardous azodye—Acid Blue 113”.
- [31] T.A. Brady, M. Rostam-Abadi, M.J. Rood*, *Gas.Sep. Purif.*, (1996) 97-102, “Applications for activated carbons from waste tires: natural gas storage and air pollution control”.
- [32] Hsisheng Teng, Michael A. Serio*, Marek A. Whjtowicz, Rosemary Basilakis, Peter R. Solomon, *Ind. Eng. Chem. Res.*, 34(1995) 3102-3111, “Reprocessing of Used Tires into Activated Carbon and Other Products”.
- [33] Zhiwei Peng, Jiann-Yang Hwang, Joe Mouris, Ron Hutcheon, Xiaodi Huang, *ISIJ International*, 50 (2010) No. 11 1590–1596, “Microwave Penetration Depth in Materials with Non-zero Magnetic Susceptibility”.
- [34] Guoqiang Lia*, Michael A. Stubblefield, Gregory Garrick, John Eggers, Christopher Abadie, Baoshan Huang, *Cement and Concrete Research*, 34 (2004) 2283–2289, “Development of waste tire modified concrete”.
- [35] Hsisheng Teng, Yu-Chuan Lin, Li-Yeh Hsu, *Air & Waste Management Association*, (2000) 1940-1946, Production of Activated Carbons from Pyrolysis of Waste Tires Impregnated with Potassium Hydroxide”.
- [36] N. Segre, I. Joekes*, *Cement and Concrete Research*, 30 (2000) 1421-1425, “Use of tire rubber particles as addition to cement paste”.
- [37] V.K. Sharma*, F. Fortuna, M. Mincarini, M. Berillo, G. Cornacchia, *Applied Energy*, 65 (2000) 381-394, “Disposal of waste tyres for energy recovery and safe environment”.
- [38] Xianwen Dai*, Xiuli Yin, Chuangzhi Wu, Wennan Zhang, Yong Chen, *Energy*, 26 (2001) 385–399, “Pyrolysis of waste tires in a circulating fluidized-bed reactor”.

[39] J.M. Valente Nabais*, P.J.M. Carrott, M.M.L. RibeiroCarrott, J.A. Menendez, *Carbon*, 42 (2004) 1315–1320, “Preparation and modification of activated carbon fibres by microwave heating”.

Appendix I

Table 7. Summary of Experimental Results of Tire rubber at 915MHz under Stagnant Air

Temperature(°C)	relative dielectric constant(ϵ')	relative dielectric loss factor(ϵ'')	$\tan\delta$
23	12.2	2.1018	0.1722
49	12.84	2.9658	0.231
74	14.14	4.6523	0.329
98	15.42	6.4732	0.4197
122	16.54	8.447	0.5108
146	17.44	9.7368	0.5584
170	18.22	11.1183	0.6101
196	19.07	12.063	0.6327
220	19.61	12.5649	0.6409
245	20.68	14.5048	0.7013
269	21.73	17.6314	0.8815
294	23.6	22.361	0.9475
319	23.89	30.2314	1.2652
345	20.25	66.1514	3.2675
366	42.92	143.8636	3.3521
391	97.33	50.6386	0.5203
415	77.77	18.4572	0.2373
444	97.81	25.7013	0.2628
469	114.88	26.8437	0.2337
493	130.88	23.9169	0.1827
517	148.58	24.0871	0.1621
543	172.34	31.0841	0.1804
568	202.16	42.391	0.2097
592	253.46	55.1766	0.2177
616	306.46	83.1038	0.2712
642	384.82	159.9935	0.4158
666	339	98.29	0.2899
691	347.04	100.1227	0.2885
716	371.89	179.7542	0.4833

Appendix II

Table 8. Summary of Experimental Results of Tire rubber at 2466MHz under Stagnant Air

Temperature(°C)	relative dielectric constant(ϵ')	relative dielectric loss factor(ϵ'')	$\tan\delta$
23	11.52	1.4701	0.1276
48	11.88	2.0008	0.1684
73	12.68	3.018	0.238
97	13.52	4.1417	0.3064
120	14.3	5.2848	0.3695
144	14.79	6.1232	0.4141
167	15.4	6.912	0.4488
194	15.77	7.3042	0.4631
219	16.28	8.3446	0.5125
243	17.38	8.8384	0.5087
267	17.97	10.8303	0.6026
292	19.31	13.0979	0.6783
317	20.63	17.2667	0.8368
342	20.7	33.535	1.6204
364	16.21	78.1551	4.8227
385	64.6	60.27	0.933
408	70.72	33.0603	0.4675
440	83.22	49.0252	0.5891
464	101.79	60.3859	0.5932
488	124.34	78.9801	0.5596
513	146.03	95.8037	0.5409
538	170.02	114.7251	0.5635
562	189.04	156.2437	0.6069
586	221.36	191	0.7058
610	241.86	8937	0.7934
635	254.95	252.2396	0.9894
652	290.97	175.5737	0.6034
684	310.37	169.3495	0.5456
708	326.01	188.4739	0.5781

Appendix III

Table 9. Summary of Experimental Results of Tire Rubber at 915MHz under UHP Nitrogen

Temperature(°C)	relative dielectric constant(ϵ')	relative dielectric loss factor(ϵ'')	$\tan\delta$
24	11.73	2.008	0.1706
50	12.13	2.5232	0.208
75	12.79	3.3812	0.2644
99	13.51	4.2661	0.3158
123	14.39	5.4601	0.3795
147	15.32	6.741	0.4399
172	16.02	7.8663	0.491
197	16.75	9.075	0.5419
222	17.19	10.0049	0.582
247	18.06	10.9282	0.605
270	19.1	11.6533	0.6101
295	19.76	13.3418	0.675
319	19.59	15.3957	0.7858
345	21.41	18.5795	0.8676
370	23.25	22.2098	0.9551
391	48.84	38.2022	0.7821
412	67.47	28.3865	0.4207
437	34.8	1.8036	0.0518
466	26.69	0.5826	0.0218
489	26.59	0.5748	0.0216
514	25.46	0.4954	0.0195
539	24.03	0.4253	0.0177
564	22.45	0.3658	0.0163
588	20.62	0.3269	0.0159
612	18.71	0.3098	0.0166
637	17.42	1.8392	0.1056
661	16.46	3.5607	0.2164
685	16.67	6.3577	0.3814
710	16.72	11.0657	0.662

Appendix IV

Table 10. Summary of Experimental Results of Tire Rubber at 2466MHz under UHP Nitrogen

Temperature(°C)	relative dielectric constant(ϵ')	relative dielectric loss factor(ϵ'')	$\tan\delta$
24	10.81	1.3766	0.1273
50	11.04	1.6982	0.1539
74	11.42	2.2113	0.1936
97	11.87	2.7429	0.2311
121	12.41	3.4796	0.2804
145	12.98	4.1952	0.3233
169	13.46	4.9016	0.3642
196	13.83	5.4595	0.3948
220	14.32	6.0416	0.4218
245	14.82	6.5463	0.4416
268	15.14	7.2044	0.4759
293	15.71	8.106	0.5161
317	15.75	8.8367	0.5611
342	15.9	10.8487	0.6825
367	16.21	12.4973	0.7709
388	26.66	26.8303	1.0064
409	38.89	36.1933	0.9307
430	34.91	5.5889	0.1601
457	27.34	1.8864	0.069
484	27.38	1.9614	0.0716
509	26.34	1.7061	0.0648
534	25.09	1.4496	0.0578
558	23.56	1.2047	0.0511
582	21.8	1.0032	0.046
606	19.9	0.8676	0.0346
630	18.16	1.4978	0.0825
654	16.39	2.5433	0.1552
678	16.18	4.2457	0.2624
702	16.74	6.6015	0.3943